



Published in final edited form as:

*J Mater Chem B*. 2020 March 04; 8(9): 1801–1822. doi:10.1039/c9tb01849b.

## Artificial Small-Diameter Blood Vessels: Materials, Fabrication, Surface Modification, Mechanical Properties, and Bioactive Functionalities

Dongfang Wang<sup>†,a,b,c,d</sup>, Yiyang Xu<sup>†,a,b</sup>, Qian Li<sup>\*,c,d</sup>, Lih-Sheng Turng<sup>\*,a,b</sup>

<sup>a</sup>Department of Mechanical Engineering, University of Wisconsin, Madison, WI, USA

<sup>b</sup>Wisconsin Institute for Discovery, University of Wisconsin, Madison, WI, USA

<sup>c</sup>School of Mechanics and Engineering Science, Zhengzhou University Zhengzhou 450001, P. R. China

<sup>d</sup>National Center for International Research of Micro-Nano Molding Technology Zhengzhou University, Zhengzhou 450001, P. R. China

### Abstract

Cardiovascular diseases, especially ones involving narrowed or blocked blood vessels with diameters smaller than 6 millimeters, are the leading cause of death globally. Vascular grafts have been used in bypass surgery to replace the damaged native blood vessels for treating severe cardio- and peripheral vascular diseases. However, autologous replacement is not often available due to prior harvesting or the patient's health. Furthermore, autologous harvesting causes secondary injury to the patient at the harvest site. Therefore, artificial blood vessels have been widely investigated in the last several decades. In this review, the progress and potential outlook of small-diameter blood vessels (SDBVs) engineered *in vitro* are highlighted and summarized, including material selection and development, fabrication techniques, surface modification, mechanical properties, and bioactive functionalities. Several kinds of natural and synthetic polymers for artificial SDBVs are presented here. Commonly used fabrication techniques, such as extrusion and expansion, electrospinning, thermal-induced phase separation (TIPS), braiding, 3D printing, hydrogel tubing, gas foaming, and a combination of these methods, are analyzed and compared. Different surface modification methods, such as physical immobilization, surface adsorption, plasma treatment, and chemical immobilization, have been investigated and are compared here as well. Mechanical requirements of SDBVs are also reviewed for long-term service. *In vitro* biological functions of artificial blood vessels, including oxygen consumption, nitric oxide (NO) production, shear stress response, leukocyte adhesion, and anticoagulation, are also discussed. Finally, we draw conclusions regarding current challenges and attempt to identify future directions for the optimal combination of materials, fabrication methods, surface modifications, and biofunctionality. We hope that this review can assist with the design, fabrication, and application of SDBVs engineered *in vitro* and promote future advancements in this emerging research field.

\*\_turng@engr.wisc.edu, Phone: (608) 262-0586.

†These two authors contributed equally to this work.

### CONFLICTS OF INTEREST

There are no conflicts of interest to declare.

## 1. INTRODUCTION

Artery disease is a major cause of morbidity worldwide, especially when blood vessels with diameters smaller than 6 millimeters are involved. Every year, healthcare costs for patients with cardiovascular diseases exceed \$300 billion per year.<sup>1</sup> At present, autologous bypass surgeries are performed clinically to create a detour around the blockage. However, the procedure can cause further injury to patients.<sup>2</sup> Also, suitable autologous grafts are not often available due to prior harvesting or the patient's health. Therefore, it is particularly important to develop artificial small-diameter blood vessels (SDBVs).<sup>3</sup> Tissue-engineered small-diameter vascular grafts with suitable mechanical and biological properties comparable to natural blood vessels provide an excellent solution for this problem, but their design and manufacture still remains a challenge.<sup>4</sup> In recent decades, more and more researchers and companies have investigated and developed various materials and methods in an attempt to fabricate SDBVs *in vitro*.<sup>5–10</sup>

As shown in Fig. 1, for SDBVs engineered *in vitro*, significant efforts have been made to address five critical aspects including materials,<sup>6</sup> fabrication,<sup>11</sup> surface modification,<sup>12</sup> mechanical properties,<sup>13</sup> and bioactive functionalities.<sup>14</sup> Based on natural, synthesized, and hybrid polymers consisting of degradable and non-degradable materials, various processing methods and composites have been employed to construct SDBV grafts. Examples of processing methods include extrusion and expansion, electrospinning, thermal-induced phase separation (TIPS), braiding, 3D printing, hydrogel tubing, gas foaming, and a combination of these methods. Proper processing and surface modification techniques are a key factor in creating an ideal microstructure and functional surface that can promote rapid endothelialization.<sup>15</sup> Also, mechanical properties—including the modulus, nonlinear elasticity, compliance, burst pressure, and suture retention strength—must match those of host tissues because a slight mechanical mismatch between the SDBV graft and the host tissue will result in eventual transplantation failure.

The physicochemical characteristics of the biomaterials' surfaces determine the interactions between the cells and the substrates. However, some materials present difficulties in constructing biomimetic microenvironments for regulating cellular events.<sup>16</sup> Surface properties and special functional domains of grafts promote interactions between cells and the substrate. A variety of surface modification methods have been employed to functionalize scaffold surfaces for cell adhesion, cell growth, cell migration, rapid endothelialization, and long-term anticoagulation properties, thereby conferring arterial-specific functions to the resultant SDBVs.<sup>5,17,18</sup>

In this review, we strive to offer a comprehensive description of the current knowledge base and challenges in order to predict the future direction of SDBV grafts. We start with a brief overview of SDBVs engineered *in vitro*. Thereafter, the progress of the materials selection and development, fabrication techniques, surface modification, mechanical properties, and bioactive functionalities are analyzed and summarized. Based on current studies, the challenges and future directions for the fabrication and bio-characterization of SDBVs engineered *in vitro* are discussed.

## 2. MATERIAL SELECTION

### 2.1. Natural and Hybrid Polymers as SDBV Grafts

Various natural and synthetic polymers have been used to fabricate SDBVs.<sup>19</sup> The natural and synthetic polymers with good biocompatibilities that are the most widely used are summarized in Table 1.<sup>20</sup> Natural polymers, including collagens,<sup>21</sup> elastin,<sup>22</sup> fibrinogens,<sup>23</sup> polysaccharides,<sup>24</sup> chitosan,<sup>25</sup> and cellulose,<sup>26</sup> are usually formed during the growth cycles of all organisms and constitute the majority of the native extracellular matrix (ECM).<sup>24,27,28</sup> ECM provides structure and mechanical integrity to living tissues, as well as providing communication with cellular components and promoting cell adhesion, proliferation, and tissue recovery.<sup>20,28</sup>

Collagen, the major tissue component that makes up several body parts including blood vessels, ligaments, skin, and muscles, is one of the most commonly used natural polymers.<sup>29</sup> By using collagen, Jiang et al. fabricated grafts via electrospinning and implanted them into arterial vessels. The results showed good biocompatibility, and the grafts effectively promoted the growth, migration, and proliferation of human umbilical vein endothelial cells (HUVECs).<sup>30</sup> In another case, by using hybrid collagen/elastin, a three-layered vascular graft was prepared. After being cross-linked and heparinized, the burst pressure of the grafts reached up to 400 mm Hg. Furthermore, the grafts presented good hemocompatibility and did not evoke platelet aggregation *in vitro*.<sup>31</sup> However, the degradation rate of the collagen and elastin was too fast, and the mechanical properties were not enough to support the flow of blood, which is consistent with pure scaffolds made of gelatin, silk, eggshell, chitosan, and other materials.<sup>10</sup>

To prolong the degradation time and improve the mechanical properties, hybrid materials have been developed and tested as SDBVs by combining synthetic polymers and natural proteins. Vascular grafts were fabricated via co-electrospinning of hybrid materials poly(D,L-lactic acid-co-glycolic acid) (PLGA), gelatin, and  $\alpha$ -elastin.<sup>32</sup> The results showed that no local or systemic toxic effects were observed when the grafts were implanted *in vivo*. In addition, the mechanical properties and tissue composition of the scaffolds were similar to native vessels.<sup>33</sup>

### 2.2. Synthetic Polymers as SDBV Grafts

Considering the limitations of natural polymers, such as cost, limited supplies, batch-to-batch variation, and cross contamination, synthetic polymers, including biodegradable polymers and non-degradable polymers, have been rapidly developed in the last decades as biomaterials. They have suitable degradation rates and by-products, adequate mechanical properties, and thermal stability, thereby addressing several key requirements for biological applications.<sup>62</sup> When engineering and fabricating SDBVs *in vitro*, synthetic biopolymers are required to provide well-controlled macromolecular structures and surface properties to support cell growth, migration, and proliferation, all without inflammation or immune reactions *in vivo*.<sup>63</sup> In general, tissue engineering biodegradable grafts and non-degradable grafts are two kinds of typical SDBVs. With the proper microstructure, mechanical properties, and biocompatibility, they have the potential to be used as artificial blood vessels.

For both natural and synthetic polymers, bioactivity can be further improved via surface modification methods to graft functional biomolecules onto the SDBVs for improved functionality.

**2.2.1 Biodegradable polymers in tissue engineering**—To investigate their suitability in vascular engineering applications, including SDBVs, all kinds of biodegradable polymers have been used for tissue engineering materials to promote tissue regeneration while retaining the ability to be degraded by the host tissue.<sup>64</sup> Tissue engineering materials have been regarded as safe and promising candidates for *in vivo* grafts due to their non-toxic degradation products.

Compared to natural polymers and proteins, synthetic tissue engineering materials have been widely studied due to their good biocompatibility, suitable degradation rate, and sufficient mechanical properties.<sup>65</sup> When vascular grafts fabricated with polyglycolic acid (PGA) were implanted into the arterial system with the help of a biomimetic perfusion system, they remained patent *in vivo* for up to 1 month.<sup>54</sup> Although PGA fibers show good biocompatibility, their acidic breakdown products can induce an inflammatory response. Other tissue engineering materials that have slow degradation rates, non-toxic degradation products, and good mechanical properties, such as polycaprolactone (PCL), polylactic acid (PLA), thermoplastic polyurethane (TPU),<sup>33</sup> poly(glycerol sebacate) (PGS), and copolymers of poly(lactic-co-glycolic acid) (PLGA), have also been tested in SDBV grafts, and have exhibited good patency rates for several months.<sup>10,33,66</sup> Although these materials have good biocompatibility, their surfaces present difficulty in constructing the biomimetic nanostructure needed for regulating cellular events.<sup>67</sup> Therefore, to improve their surface properties and provide a special functional domain for *in vitro* grafts, some surface modification methods for grafting biomacromolecules and receptors have been employed to promote cell adhesion, growth, migration, and proliferation. However, the cellular toxicity of the breakdown products of those materials has not been comprehensively reported and should be investigated in long-term studies.<sup>68</sup>

The degradation rate also plays a critical role in maintaining the long-term function of SDBV grafts.<sup>69–80</sup> Fast degradation, which may take only hours,<sup>75</sup> impairs cell attachment, cell proliferation, and endothelialization. However, slow degradation, which may take more than 1 year,<sup>72,80</sup> prolongs the process of blood vessel regeneration. Table 2 summarizes the degradation period of commonly used biodegradable polymers for SDBV applications. The shortest degradation period was one month and the longest one could reach two years. And for collagen, the degradation period was only 5 hours. For better bio-function match, the degradation rate should be carefully decided based on the patient's health condition as well as the specific blood vessel to be replaced.

Due to their good biocompatibility and mechanical properties, more and more research has focused on the construction of SDBV grafts using hydrogels, including polyacrylamide (PAM),<sup>43</sup> polyvinyl alcohol (PVA),<sup>81</sup> gelatin methacryloyl (GelMA),<sup>45</sup> gelatin, collagen, polyethylene glycol (PEG),<sup>82</sup> and chitosan.<sup>25</sup> Remarkably, GelMA, a semi-synthetic hydrogel consisting of gelatin derived with methacrylamide and methacrylate groups, has attracted attention in the application of SDBV grafts recently by virtue of its suitable

biological properties, tunable mechanical properties, and good physical characteristics.<sup>83</sup> Due to the presence of cell-attached and matrix metalloproteinase-responsive peptide motifs, GelMA hydrogels present some essential properties of native ECM that allow cells to proliferate and spread in the hybrid hydrogel systems formed by mixing GelMA with other biofunctional biomaterials.<sup>44</sup>

**2.2.2 Non-degradable polymers**—Biostable polymers, such as expanded polytetrafluoroethylene (ePTFE) and polyethylene terephthalate (PET), are currently the standard biomaterials for vascular grafts in clinical applications. They perform well as large-diameter blood vessel grafts (>6 mm)<sup>84,85</sup> and have been widely used in humans since the 1970s.<sup>86</sup> PET, as a large-diameter artificial blood vessel graft, was first implanted *in vivo* by Julian in 1957.<sup>87</sup> Because the surfaces of PET and ePTFE are electronegative, they have good stability and do not undergo biological deterioration *in vivo*, which minimizes their reaction with blood components. For large-diameter blood vessel graft applications, the larger flow area, higher rate of blood flow, and relatively inert properties of PET and ePTFE decrease the possibility of thrombosis and restenosis; thus, the grafts can maintain long-term stability.<sup>88</sup> However, the development of a replacement for SDBV is still a challenge<sup>58</sup> because they tend to fail by occlusive thrombi due to the lower blood flow rate. Moreover, the mechanical mismatch between the material and the host tissue, as well as the chronic foreign body response around the graft, may limit blood vessel functionality and promote cell hyperplasia.<sup>64,89</sup> Consequently, more and more researchers are looking for new potential methods for constructing SDBVs using ePTFE, including manufacturing methods,<sup>90,91</sup> material blends,<sup>55</sup> surface modifications,<sup>92</sup> and stem cell differentiation.<sup>18</sup>

### 3. FABRICATION METHODS

There are many promising fabrication methods for manufacturing SDBVs with matching mechanical properties, such as paste extrusion followed by expansion (specifically for ePTFE), electrospinning, TIPS, braiding, 3D printing, synthesis of hydrogels, gas foaming, and combinations of these fabrication methods. In this section, we discuss different ways to fabricate grafts. By the optimal combination of materials and fabrication methods, grafts engineered *in vitro* with desirable structures, properties, and bio-functions have been developed.

#### 3.1. Paste Extrusion and Expansion

Paste extrusion and expansion are the traditional techniques used to fabricate ePTFE artificial blood vessels, as shown in Fig. 2. In 1969, Gore patented and manufactured ePTFE by means of a mixing, extrusion, heating, and expanded stretching process, which yielded a microporous structure that was beneficial for tissue adhesion in vascular grafts.<sup>84,93,94</sup> The typical structure of ePTFE is a node–fibril structure, where the solid nodes connect through fine fibrils with an average internodal distance of 30  $\mu\text{m}$ , which is similar to the size of endothelial cells.<sup>90</sup> Due to its successful application in large-diameter artificial blood vessels in recent years, how to effectively improve the process for fabricating novel ePTFE SDBV grafts has been gaining more and more attention.

Nowadays, many novel processes, including blending, jet-blowing, and thermo-mechanical stretching, have been adopted to prepare ePTFE membranes.<sup>95–97</sup> The morphology and porosity are the two critical parameters that influence the final performance of ePTFE because the morphology affects the mechanical strength and the structure, which need to be suitable for endothelial cell adhesion and growth.<sup>90</sup> The porosity, which is the distance and space between nodes formed during thermo-mechanical stretching, affects blood transport and permeability.<sup>98</sup> When the internodal distance is higher than 45  $\mu\text{m}$ , the capillaries can traverse the prosthetic vascular wall.<sup>99</sup> By adjusting the manufacturing process or inducing appropriately selected crystal disorders, the morphology of the fibrillated structure and membranes with fibril lengths can be controlled.<sup>90</sup>

Another important issue is the orientation of the nodes and fibers. Currently, the fiber direction of the majority of vascular grafts is parallel to the direction of the blood flow, and the direction of the nodes is aligned along the circumference. It has been reported that electrospun fiber membranes oriented along the direction of the blood flow can promote endothelial cell orientation along the axial direction. Whether the fiber structure of ePTFE is beneficial for EC orientation along the bloodstream due to the existence of nodes has not yet been proven. Constructing a node structure along the axial direction and investigating the influence of the node–fiber structure on endothelial cells (ECs) may be the next key issue. Mixing adequate lubricating agents (lubricants) was useful for ePTFE fabrication; however, many lubricants, including mineral oil, naphtha, and soy bean oil, were either toxic or difficult to remove after extrusion,<sup>91</sup> thus limiting their application in the field of SDBVs. Thus, the development of new lubricants for benign processing is an urgent problem to be solved. This will provide a chance to fabricate biofunctional ePTFE, which is beneficial for cell growth and proliferation.

### 3.2. Electrospinning

Electrospinning was first reported by Gilbert.<sup>89</sup> It is an electrostatically driven process for making nanofibers with high surface areas, fine porosities, and tunable mechanical properties, as well as being a simple and cost effective fabrication process.<sup>100,101</sup> Typical electrospinning equipment consists of a syringe pump, collector, and high-voltage supply, as shown in Fig. 3A. In the last decades, it has been widely explored to construct novel membranes and scaffolds with different structures by controlling the material solutions, process parameters, and/or through design of new collectors.<sup>102,103</sup>

The fiber structures can be influenced by several material and processing parameters,<sup>104</sup> including the solution,<sup>81</sup> process,<sup>105</sup> and external ambient environment.<sup>106,107</sup> Solution parameters are an inherent property of the material and solvent, such as the nature of the solvent, molecular weight, viscosity, concentration, and surface tension. Processing parameters are determined by the instrument set-up and include the voltage, working distance, flow rate, and the design of collectors. The temperature and humidity determine the ambient parameters. Generally, low solution concentrations, high material molecular weights, high solution flow rates, and small working distances will generate smaller fiber diameters.<sup>106</sup>

Due to the inherent properties of the material, different microstructures can be obtained by designing new collectors and/or using coaxial and tri-axial needles.<sup>108</sup> As shown in Fig. 3B, aligned fibers and orthogonal, woven-net-structure fibers can be obtained by using a conductive rotation drum or two parallel conductive plates, and four orthogonal conductive plates, respectively.<sup>106</sup> Also, composite materials have been created by adding functional biomaterials to synthetic tissue engineering materials, which have then been used for electrospinning to improve biocompatibility.<sup>35,38</sup> Furthermore, by using a customized electrospinning collector, a vascular graft with a layered, circumferentially aligned, and micro-wavy fibrous structure similar to natural elastic tissues was fabricated (Fig. 3C).<sup>109</sup> In addition, by using a three-step electrospinning method,<sup>110</sup> a tri-layer vascular graft consisting of aligned inner layer fibers, yarns in the middle layer, and random fibers in outer layer was fabricated. The tri-layer structure provided tensile and compressive mechanical support, while the biological results revealed improved biocompatibility and tissue regenerative capabilities.<sup>111</sup> Also, Jiang et al. loaded synthesized vascular endothelial growth factor (VEGF) nanoparticles into a polycaprolactone (PCL) solution for electrospinning to regulate the differentiation of stem cells into endothelial cells.<sup>30</sup> Furthermore, an artificial vascular graft was fabricated using a coaxial electrospinning method that can simply load the anticoagulant heparin, and the structure can control the release profile of the heparin. Adding growth factor contributed to promoting human umbilical vein endothelial cell (HUVEC) growth and improved the blood compatibility of the graft (Fig. 3D).<sup>112</sup>

### 3.3. Thermal-Induced Phase Separation (TIPS)

The principle of TIPS is to phase separate a polymer–solvent or polymer–solvent–non-solvent homogeneous solution by cooling it to a low temperature to introduce polymer-rich and polymer-lean phases. After induced phase separation, the solvent is removed by extraction, evaporation, or freeze drying, and pores are formed in the remaining solid phase due to solvent removal.<sup>113</sup> There are two typical TIPS mechanisms; namely, solid–liquid phase separation and liquid–liquid phase separation.<sup>106</sup> TIPS has been adopted to construct biodegradable scaffolds including blood vessel grafts. A micro-tubular orientation-structured blood vessel mimicking a natural structure was prepared by an improved TIPS technique. The process parameters—such as the environmental temperature, temperature gradient, and concentration of the polymer solution—were found to affect the structure and morphology of the resultant vessel grafts.<sup>47</sup> Furthermore, by utilizing the differences in thermal conductivities of mold materials, oriented gradient microtubular structures in the axial or radial direction were fabricated using benzene as the solvent, which can also facilitate blood vessel regeneration (Fig. 4A).<sup>114</sup> Moreover, by combining the braiding and TIPS methods, a biodegradable tubular scaffold was prepared, with the tube fabricated using a braiding machine and the coating on the braided tube surface made via TIPS.<sup>46</sup>

### 3.4. Braiding

Braiding is a process of winding three or more fiber yarns in a specific pattern along the direction of fabric formation (Fig. 4B).<sup>115,116</sup> The low bending stiffness of the braided tube, and the ease of compression and recoil of the braided structure, make them promising candidates for SDBVs.<sup>117</sup> However, since the required stitching of the tubular graft limits

the movement of the constituent lines at their intersection, the braided graft has not been very successful in endograft applications.<sup>118</sup> Thus, the concept of using a multi-layer weave design has been introduced to reduce the porosity of the graft while maintaining flexibility, and it has been used to make novel vascular grafts. By braiding, flattening, and winding the silk fibers onto a cylindrical polymer tube and then coating it with an aqueous silk fibroin solution, Yasumoto et al. constructed a SDBV graft with an inner diameter of 1.5 mm and a length of 10 mm. After implantation into the abdominal aorta of rats, endothelial cells and smooth muscle cells (SMCs) migrated early into the silk fibroin grafts and organized into endothelial cells and smooth muscle layers (Fig. 4C).<sup>119</sup> In addition, poly(lactic-co-glycolic acid) (PLGA) nanoparticles were covalently immobilized on the braided form of a crimped polyethylene terephthalate (PET) cardiovascular graft to treat early thrombosis and inflammation, resulting in low cytotoxicity and good biocompatibility.<sup>116</sup>

### 3.5. 3D Printing

Three-dimensional (3D) printing—converting a 2D volumetric digital image into a 3D printed model via printing successive thin layers of material—has been around for several decades.<sup>120</sup> Due to the quickly customizable and personalized organ-like products created by 3D printing or bioprinting,<sup>121</sup> more attention has been paid to using it for the fabrication of SDBV grafts. Stefan et al. developed a new resin formulation containing cyanoethyl acrylate, which has good mechanical properties and biocompatibility. Furthermore, the resin was printed by microlithography for SDBVs (Fig. 4D).<sup>122</sup> By using poly(propylene fumarate) (PPF), Melchiorri et al. printed a vein graft designed to fit the specific curvature of a patient's anatomy, which was subsequently tested for fluid dynamics before eventual 3D fabrication of the customized implant.<sup>122</sup> Three-dimensional printing is a promising tool for generating tissue-engineered scaffolds using different target cells in biocompatible materials (e.g., hydrogels). However, 3D printing has not been directly applied to the generation of patient-specific coronary artery bypass grafts. Most studies have focused on the *in vitro* production of vascular models and the lining of endothelial cells on the inner surface; in particular, the formation of microvascular networks to study angiogenesis and thrombosis or the supply of nutrients and oxygen to engineered tissues.<sup>123</sup>

### 3.6. Hydrogels as Grafts

Due to the good biocompatibility and mechanical properties of hydrogels, more and more research has focused on the construction of SDBV grafts using hydrogels. A highly stretchable hydrogel tube as a potential artificial blood vessel was fabricated, and heparin-grafted dopamine was immobilized on an alginate/polyacrylamide (PAM) double-network hydrogel via a mussel-inspired coating. The results demonstrated enhanced anticoagulant activity, hemocompatibility, and an improved cell adhesion affinity towards blood endothelial cells (EC).<sup>124</sup> Polyvinyl alcohol (PVA) hydrogel, a water-soluble synthetic polymer, was used to construct vascular grafts by the copolymerization of PVA with dextran, and the grafts improved blood–biomaterial interactions while inhibiting thrombogenicity (aka platelet adhesion).<sup>125</sup> Also, by coating the electrospun nanofiber tubes with PVA hydrogel, dual-network composite scaffolds were fabricated, and the results indicated that the cell viability and mechanical properties improved.<sup>61</sup> Remarkably, by using gelatin methacryloyl (GelMA)-encapsulating ECs, the cells were homogeneously located on the



lumen of small-diameter tubular scaffolds consisting of PCL with a GelMA inner layer, thus achieving 3D endothelialization.<sup>45</sup>

### 3.7. Gas Foaming

Gas foaming, which is a method that generates porous structures by the expansion of gas, includes batch foaming, microcellular injection molding, and extrusion foaming.<sup>106,126</sup> The principle is that the dissolved gas (CO<sub>2</sub> or N<sub>2</sub>) in the polymer in the supercritical state has good miscibility with the polymer. When the high pressure is released, the dissolved gas emerges and turns into the gaseous state. Then, a porous structure is formed by gas nucleation and expansion.<sup>106</sup> A gas-foaming method was used to create macro-scale pores in macroporous calcium phosphate cement, and the results indicated that microcapillary-like structures formed in the scaffolds.<sup>126</sup> By mixing polycaprolactone/poly(lactic acid) (PCL/PLA) blends, highly interconnected porous polymer scaffolds were prepared by gas foaming using CO<sub>2</sub> as the physical blowing agent. The interconnected porous structure may provide a chance to fabricate SDBV grafts *in vitro*.<sup>127</sup> A similar method was used to fabricate a small-diameter tubular PCL/PLA foamed scaffold, and the human umbilical vein endothelial cells (HUVECs) cultured on the surfaces of the PCL/PLA scaffolds showed high viability and migration.<sup>128</sup> However, since the cells produced by gas foaming were mostly closed-cell structures, the connectivity was poor; hence, the use of gas foaming to construct vascular grafts is limited. If the cell connectivity and flexural modulus can be enhanced, then the efficiency of preparing blood vessel grafts via gas foaming will be greatly improved.

### 3.8. Combination of Fabrication Methods

There are many methods of making SDBVs, such as the various methods described above. However, due to the limitations of a single processing method to fabricate multi-functional SDBV grafts, a combination of various fabrication methods have been studied and developed.

By combining electrospinning and braiding, a tubular graft with mechanical properties that closely matched the layers of native blood vessels was manufactured. Electrospinning provided the fabrication of fibers in the micro- to nanometer size that mimicked the structure of the native ECM, while braiding provided the suitable mechanical properties.<sup>42</sup> Mi et al. fabricated triple-layered small-diameter vascular scaffolds composed of silk and thermoplastic polyurethane (TPU) by combining braiding, electrospinning, and TIPS methods. The resulting vascular grafts were composed of an inner nanofibrous layer, middle woven-silk filament layer, and outer porous layer that mimicked the structure of native blood vessels. The desirable toe region, sufficient suture retention, and burst pressure were suitable for vascular graft applications, and an endothelial cell layer was present on the inner surface of the scaffold with favorable morphology (Fig. 5A).<sup>129</sup>

Sang et al. fabricated an artificial blood vessel graft composed of a mixture of chitosan and polycaprolactone (PCL) nanofibers coated with PCL strands by electrospinning and 3D printing. The results presented excellent mechanical properties and indicated that the method could be used for revascularization (Fig. 5B).<sup>130</sup> Similarly, a novel three-layer vascular graft that mimicked the structure of natural blood vessels was made by E-jet 3D printing and

electrospinning. The results indicated that the function of the vascular lumen surface could be expressed *in vivo* by the novel grafts (Fig. 5C).<sup>13</sup>

By electrospinning poly (L-lactic acid) (PLLA)/gelatin outside of the decellularized vessels, a bilayer tissue-engineered vascular graft was prepared, and the outer layer was functionalized by immobilizing heparin. The results showed that the grafts were still patent with no expansion or aneurism after four weeks of implantation, and the inner surface formed a monolayer of cells, forming a dense intermediate layer. The mechanical properties of the regenerative vessels were similar to those of a rat abdominal aorta (Fig. 5D).<sup>42</sup> Furthermore, to obtain the formation of the ECM structure, a 3D nanofiber complex scaffold with cells was constructed via a combination of electrospinning and origami techniques that promoted cell growth and migration.<sup>131</sup>

## 4. SURFACE MODIFICATION

Although porous scaffolds with well interconnected pores and suitable mechanical properties are sufficient to allow cell infiltration, their surface characteristics (e.g., hydrophilic/hydrophobic properties based on the chemical composition) may not satisfy all the needs of cell adhesion, migration, and proliferation.<sup>132</sup> In order to improve the surface biocompatibility of implantable biomaterials, attempts have been made to mimic the natural extracellular matrix by immobilizing bioactive molecules to the scaffold surface through surface modification.<sup>133</sup> Surface modifications have been applied to functionalize the grafts in such a way that it promotes the cascade of biological events that ultimately regenerate or repair/replace diseased tissues with functional tissues. Biological functionalization of the surface is a popular research topic that relies on biological tools to create biomimetic surfaces with biologically active or inactive molecules to produce specific responses.<sup>12</sup> In recent years, many modification methods, including physical immobilization, surface adsorption, plasma treatment, and chemical immobilization, have been developed to graft various functional biomacromolecules onto the surface, such as growth factors, DNA, or drugs, thereby promoting cell adhesion, growth, migration, and differentiation, as well as angiogenesis, anticoagulation, and tissue regeneration (cf. Table 3).<sup>12,134</sup> In this section, we mainly discuss the progress of four surface modification methods used in recent years, including physical immobilization, layer-by-layer (LbL) self-assembly surface adsorption, plasma treatment, and chemical immobilization.

### 4.1. Physical Immobilization

Since physical immobilization can completely retain the biological activity of biomacromolecules, and it is non-toxic and simple to prepare, it has been widely applied to modify and optimize surface properties of cardiovascular grafts.<sup>12</sup> For example, polyethylene glycol (PEG) and chitosan were blended and their physical and chemical properties, mechanical strength, and thermodynamic attributes were studied. The results indicated that the optimum PEG concentration helped to maintain the natural structure of the protein adsorbed on the surface, which was beneficial for cell adhesion, growth, and proliferation.<sup>51</sup> Heparin, as an anticoagulant and polyanion, was also employed in the method of physical adsorption. By immobilization onto the surface of the grafts, heparin

maintained its normal conformation and remained highly active, which was useful for improving the hemocompatibility, anticoagulation ability, and cell growth.<sup>150</sup> However, due to the weak interaction between the matrix material and the biomacro-molecule, the bioactive molecule had a burst release phenomenon, and the biological function could not be retained for an extended period of time.

#### 4.2. Layer-by-Layer (LbL) Self-Assembly Surface Adsorption

Layer-by-layer (LbL) self-assembly is a simple and versatile deposition process. It has been widely used in the fields of superhydrophobic surfaces, implant coatings, and drug-delivery devices.<sup>151</sup> Due to its good biocompatibility and the absence of chemically toxic substances, LbL has been widely used to graft peptides onto substrates to improve the surface bioprofiles of artificial SDBVs.

In order to more efficiently bind and activate angiogenic growth factors for cell signaling, Kanya et al. developed a method of nucleating nanostructures using heparin that can display these biomacromolecules on the graft surface. By mixing two liquids, including peptide amphiphile and heparin solution with VEGF, a self-assembled nanostructure with a strong angiogenic ability formed in seconds.<sup>67</sup> Similarly, dextran sulfate, heparin, and chitosan were coated on vascular grafts via self-assembly, and the anticoagulation ability and biocompatibility of the scaffold was greatly improved after modification (Fig. 6A).<sup>152</sup> By LbL self-assembly of heparin and chitosan, multi-structured vascular patches were constructed, yielding high resistance to platelet adhesion, promoting cell attachment and proliferation, and maintaining the long-term patency of surgical arteries (Fig. 6B).<sup>37</sup>

In order to construct a vascular graft with *in situ* nitric oxide (NO) generation, heparin and selenium-containing catalysts were incorporated onto the surface of the polycaprolactone (PCL) matrix by LbL assembly. Compared to PCL, the modified grafts promoted EC adhesion, growth, and proliferation, and inhibited smooth muscle cell adhesion and growth.<sup>153</sup> Furthermore, in order to improve the stability of the self-assembled coating, Jiang et al. developed a novel nanocoating where heparin and catechol-modified chitosan were used as polyelectrolytes by forming micelles with amphiphilic block copolymers functionalized with phenylboronic acid, which formed borate bonds with catechol. The interaction forces between the coating components included physical adsorption, electrostatic adsorption, covalent bonding, and hydrogen-rich bonding forces, which provided enhanced stability to the coating. The results of cell culture *in vitro* and *in vivo* showed potential for achieving enhanced re-endothelialization for vascular implants (Fig. 6C).<sup>36</sup> Similarly, to improve the stability of LbL nanocoating and promote release time, genipin was crosslinked to different gelatin and polylysine layers to form stable structures by amide bonds, with a release time of up to 60 days (Fig. 6D).<sup>16</sup>

However, an uneven distribution of natural polymers within the synthetic polymer matrix might occur due to their poor compatibility, which would result in the limitation of the natural polymer component content.<sup>154</sup> Thus, effectively improving the uniform distribution of self-assembly on the surface of the matrix material, and thereby promoting the uniform expression of biological functions and cell behavior on the surface of the graft, is critical.

### 4.3. Plasma Treatment

Plasma treatment of polymeric substrates has been widely used to improve surface wettability by changing the surface's chemical composition. Multiple functional groups can be bound to the target surface by a suitable plasma source, allowing subsequent covalent attachment of various biologically active molecules. For example, typical plasma treatments with oxygen, ammonia, or air can produce carboxyl or amine groups on the surface. A variety of proteins and peptides—such as arginylglycylaspartic acid (RGD), Arg-Glu-Asp-Val (REDV) peptide, VEGF, siRNA, heparin, and Tyr-Ile-Gly-Ser-Arg (YIGSR)—can be immobilized on plasma-treated surfaces to enhance cell adhesion, growth, migration, differentiation, angiogenesis, and anticoagulation.<sup>134</sup>

In general, the surface properties of a sample can be improved by one-step plasma treatment. Compared to the untreated samples, plasma-treated polyethylene terephthalate (PET) and polytetrafluoroethylene (PTFE) can promote the expression of cell adhesion molecules on human endothelial cells *in vitro*.<sup>59</sup> Similarly, ammonia plasma treatment of polystyrene (PS) surfaces enhances proliferation of primary human mesenchymal stem cells (MSC) and human endothelial cells.<sup>155,156</sup> To improve the blood compatibility of expanded PTFE (ePTFE), a novel method of binding the chitosan/heparin complex to the surface of the vascular graft was developed. After plasma treatment, ePTFE was immersed in the heparin solution and chitosan solution to graft molecules. The results exhibited significantly reduced platelet adhesion, and the grafts were found to still be patent two weeks post-implantation in dog veins (Fig. 7A).<sup>136</sup> Similarly, to promote anticoagulation, heparin was grafted onto the surface of the lumen of ePTFE vascular grafts after plasma treatment. *In vitro* blood compatibility experiments showed that the number of adhesive platelets on modified ePTFE vascular graft surfaces decreased sharply, thus further promoting endothelialization and inhibiting antithrombogenicity of SDBV grafts (Fig. 7B).<sup>92</sup> Also, various cell adhesive proteins—including tropoelastin and biomacromolecules—can be bound to the matrix surface after plasma immersion ion implantation. After N<sub>2</sub> plasma treatment, the surface of the PTFE was roughened with nanostructures, and the abundant free radicals generated underneath the surface continuously migrated to the surface and reacted with biomacromolecules by simple solution immersion. Thus, various biomolecules with different functions—including heparin, stromal cell-derived factor 1 (SDF-1 $\alpha$ ), and CD47—can be steadily immobilized on the surface of PTFE, which can effectively promote cell adhesion and proliferation, and inhibit platelet attachment (Fig. 7C).<sup>5,157</sup> In order to form a more stable structure on the surface of the plasma, the grafted biomolecules are further cross-linked. Mi et al. developed a mussel-inspired modification approach where oxygen plasma treatment, dopamine coating, polyethylenimine (PEI) grafting, and RGD or RGD/heparin were immobilized and crosslinked. The results indicated the simultaneous improvement of endothelial cell affinity and antithrombogenicity (Fig. 7D).<sup>60,135</sup>

### 4.4. Chemical Immobilization

When the incorporated molecules are covalently attached to the surface of vascular grafts, they can sustain slow and yet prolonged release from the substrates when incubated. Thus, such a technique is suitable for immobilizing biomacromolecules. However, it should be noted that when the grafted site is chemically modified, partial inactivation of the

immobilized molecule can occur upon covalent modification. Therefore, how to prolong the release time while ensuring the activity of biomacromolecules becomes more and more important. Remarkably, a facile surface modification method, which can be applied to a host of solid materials from natural to synthetic polymers by simple dip-coating with a dopamine solution, was reported (Fig. 8A).<sup>138</sup> Dopamine creates a stable layer that adheres to the surface of the substrate material by undergoing oxidative polymerization under slightly basic conditions. In one of the approaches, polycaprolactone (PCL) was first electrospun into nanofibers and then coated with dopamine to functionalize the nanofiber surface with numerous catechol moieties. Upon cell seeding with HUVECs, the cells showed highly enhanced adhesion and viability (Fig. 8B).<sup>48</sup> Compared with other chemical immobilization methods, the reaction environment of dopamine presented simplicity and cleanliness, while the post-modification of the resulting polydopamine (PDA) layer allowed for the functionalization of bioactive molecules containing thiols or primary amines by imine formation and/or Michael addition.<sup>56</sup> It has been shown that various biomacromolecules, such as VEGF and RGD, can be immobilized on the surface followed by PDA coating, which can enhance EC adhesion, growth, proliferation, and differentiation (Fig. 8C).<sup>158</sup> Also, elastic poly(l-lactide-co-caprolactone) (PLCL) films were first deposited with PDA, followed by immobilization with a cell-adhesive RGD-containing peptide and basic fibroblast growth factor via dip coating. The presence of multiple signaling factors synergistically accelerated EC adhesion and proliferation (Fig. 8D).<sup>137</sup> Similarly, VEGF and angiopoietin-1 were covalently immobilized onto 3D porous collagen scaffolds using 1-ethyl-3-(3-dimethylaminopropyl) carbodiimide (EDC) chemistry, which can effectively promote the formation of vascular structures.<sup>142</sup> By immobilizing organoselenium onto polyethyleneimine (PEI) and loading it onto the electrospun PCL graft, an *in situ* catalytic nitric oxide (NO) generation layer was created. Meanwhile, hyaluronic acid was grafted with an EC-specific peptide REDV and deposited onto substrates to fabricate a multi-functional layer. The results indicated that the small-diameter vascular grafts promoted EC adhesion, growth, and rapid endothelialization (Fig. 8E).<sup>141</sup>

## 5. MECHANICAL PROPERTIES

It is crucial for artificial blood vessels to emulate the mechanical properties and performance of natural blood vessels. Unfortunately, differences in sample size, test methods, tissue sources, sample processing methods, etc., can cause wide variation in mechanical properties.<sup>109,159–161</sup> For artificial SDBVs, even a slight mismatch in mechanical properties will lead to thrombosis and other potentially fatal complications. During the past decades, significant efforts have been made to improve the mechanical properties of artificial SDBVs. Here, we focus on improvements to the modulus, nonlinear elasticity, compliance measurement, burst pressure, and suture retention strength of the engineered vessels.

### 5.1. Fatigue Properties and Elastic Modulus

The modulus of elasticity or Young's modulus, defined as the stress/strain ratio in the linear region of the tensile stress–strain curve, is an inherent mechanical property of the graft material. The Young's modulus defines the stiffness of the material, even though its value may depend on the rate of elongation, and it is critically important for the application of

SDBV grafts.<sup>162</sup> Currently, many promising materials and methods have been developed to improve the mechanical properties of small-diameter vascular grafts, including composite materials, novel fabrication techniques, surface modifications, and chemical crosslinking. By electrospinning polyurethane (PU) onto a polycaprolactone (PCL) airbrushed tube, Abdalhay et al. fabricated biphasic tubular scaffolds, followed by thermal crosslinking at 60 °C to strengthen the bonding interaction between the two materials. The results showed that the tensile strength and tensile elastic modulus of the scaffolds significantly increased.<sup>163</sup> In fact, the mechanical properties, including the elastic modulus and fatigue properties, can be effectively improved by a variety of methods. Perhaps the real difficulty lies in how to construct a graft that matches the mechanical properties of a native blood vessel, because the mismatched stress will accelerate the failure of small-diameter artificial grafts as blood vessels.

## 5.2. Nonlinear Elasticity

Nonlinear elasticity, including the so-called toe region, is a very important property of native blood vessels. Human blood vessels show a low circumferential Young's modulus (usually 20–50 kPa) at the beginning of radius expansion, which indicates good flexibility. After a certain expansion (30–60% strain), the Young's modulus increases sharply, by up to 100–200 kPa,<sup>161</sup> which acts to constrain its further expansion. This property could well protect blood vessels from rupturing when there is a sharp and instant increased blood demand, such as when doing sports or during a burst of crying or laughter. This behavior relates to elastin and collagen fibers in the vessel walls. Both of these fiber types are aligned along the circumferential direction; however, collagen fibers have a curvy configuration while elastin fibers are straighter and less wavy.<sup>164</sup> At the beginning of vessel expansion, only the rubbery elastin fibers straighten and then elongate, while collagen fibers unfold, which results in a very low Young's modulus. As the expansion or strain increases, the collagen fibers begin to straighten completely, yielding a much higher Young's modulus and thus leading to a steep slope in the strain–stress curve.<sup>109</sup>

In recent years, many methods have been developed to fabricate small-diameter vascular grafts with nonlinear elasticity. By designing a customized rotating collector, Yu et al. fabricated hybrid grafts with mechanical properties comparable to natural blood vessels (cf. Fig. 3C). The results showed that a sufficient toe region and the capacity for long-term usage under repeated dilation and contraction were provided by the circumferentially aligned and wavy biomimetic configuration (Fig. 9A).<sup>109</sup> Furthermore, after modification of wavy multicomponent vascular grafts by fabricating triple-layers, the nonlinear tensile stress–strain relationship mimicked the toe region of native blood vessels, giving them sufficient mechanical strength to meet implantation requirements for tensile strength, suture retention, and burst pressure.<sup>139</sup> However, the orientation structure was along the circumferential direction. In order to obtain the aligned structure parallel to the long axis direction, Niu et al. improved the receiving device and obtained the nonlinear mechanical region by micro-stretching. With the novel receiving device and micro-stretching process, controllable fiber orientation and nonlinear elasticity of electrospun SDBV grafts for vascular tissue engineering were successfully fabricated (Fig. 9B).<sup>165</sup> Furthermore, by mimicking the multi-layered structure of native blood vessels, triple-layered vascular grafts with biomimetic

mechanical properties were successfully constructed, consisting of a braided silk fiber inner layer, polyacrylamide (PAM) hydrogel middle layer, and thermoplastic polyurethane (TPU) outer layer. Their non-linear physical property was due to the woven silk fibers (Fig. 9C).<sup>43</sup>

### 5.3. Compliance Measurements

As a measure of the elastic deformation of a material in response to pressure, compliance can be calculated according to ANSI guidelines,

$$\% \text{ compliance per 100 mmHg} = \frac{(R_{P_1} - R_{P_2})/R_{P_1}}{P_1 - P_2} \times 10^4$$

where  $P_1$  is the lower pressure value,  $P_2$  is the higher pressure value (in mmHg), and  $R_{P_1}$  and  $R_{P_2}$  are the vessel inner diameters at the respective pressures.<sup>166</sup>

When associated with a vascular structure, compliance is the dimensional change of the tube that occurs in response to pressure variations within the lumen.<sup>167</sup> The compliance mismatch between the artificial vascular graft and host artery is one of the major causes of anastomosis.<sup>9,168</sup> This is because the hemodynamic flow varies due to compliance differences across an anastomosis. This leads to an increase in shear stress, which damages endothelial cells and reduces shear stress, which leads to an increase in the relative stasis areas and interactions between platelets and the vessel wall.<sup>169</sup> The resulting difference in pressure at the anastomosis can lead to intimal hyperplasia and thrombosis.<sup>42,170</sup> To minimize these disruptive flow characteristics, many ways to match compliance of artificial blood vessels with native blood vessels have been developed, including composites, bionic structures, post-treatments, and surface modifications. By fabricating a soft polycaprolactone (PCL) matrix with a flexible polylactic acid (PLA) knitted fabric, a composite vascular graft was produced that exhibited improvements in tensile strength, burst strength, elastic recovery, and compliance.<sup>171</sup> Similarly, by combining elastic poly(l-lactide-co-caprolactone) (PLCL) in a bilayered configuration, a graft having circumferentially aligned microfibers was constructed. The grafts presented adequate suture retention strength and good compliance compared to native arteries. Most importantly, the grafts enabled the formation of new arteries.<sup>172</sup>

### 5.4. Burst Pressure Measurements

Burst pressure is the maximum pressure that a vascular vessel can withstand before an acute leak occurs and it fails. This is expressed as,

$$f = \frac{Pd}{2t}$$

where  $F$ ,  $P$ ,  $d$ , and  $t$  are the maximum force, burst pressure, diameter, and wall thickness, respectively.

Since  $f$  is a finite entity, the burst pressure decreases as the diameter increases and the wall thickness decreases. However, for a small-diameter graft, the burst pressure could be much

higher than the blood pressure. As Sarkar measured,<sup>168</sup> the burst pressure of a carotid artery is close to 5000 mmHg, while a common systolic pressure is only around 130 mmHg. Nowadays, there are many methods to fabricate *in vitro* engineered SDBV grafts that can meet the burst pressure. Porous polyurethane (PU) grafts fabricated using electrospinning have burst pressures up to 1850–2050 mmHg; much greater than any possible physiological blood pressure.<sup>168</sup> When using polycaprolactone (PCL)/collagen composites, the burst pressure of the scaffolds was  $4912 \pm 155$  mmHg, which is also much larger than that of native blood vessels.<sup>49</sup> In another case, in multilayer vascular grafts based on collagen-mimetic proteins, the compliance, burst pressure, and suture retention strength were able to match the reported values of saphenous vein autografts.<sup>7</sup> It is worth noting that *in situ* observations of relative microstructural features of failure during burst pressure have been extensively investigated and it has been found that highly oriented fibers and maximum tensile properties are not necessary to achieve clinically sufficient burst pressure data. In fact, electrospun nanofibrous blood vessels without a discernible fiber alignment can also achieve clinically sufficient burst pressures.<sup>173</sup>

### 5.5. Suture Retention Strength (SRS)

Suture retention strength (SRS) is a term that measures the adhesion of an implant to surrounding tissue. It is a key issue for surgery as its resistance to the stresses associated with implantation can only be established by determining the force necessary to pull a suture through the wall.<sup>174</sup> There are many ways to enhance SRS. Compared to single-material devices, a composite vascular graft fabricated by combining flexible polylactic acid (PLA) with a soft polycaprolactone (PCL) matrix can improve the mechanical characteristics, especially in compression and torsional resistance.<sup>55</sup> Lorenzo et al. developed an elastomeric scaffold with a novel bilayered structure that included a highly porous inner layer that allowed cell integration and growth, and an external fibrous reinforcing layer fabricated using electrospinning. The compliance and suture retention were  $4.6 \times 10^{-4}$  mmHg<sup>-1</sup> and  $3.4 \pm 0.3$  N, respectively.<sup>66</sup> However, the effects of SRS on the vascular graft microstructure have not been characterized, and how to investigate the effect of burst pressure on endothelial cell behavior *in situ* under dynamic conditions has not been explored. These are crucial for studying the effects of shear force, burst pressure, suture retention strength, and compliance on endothelial cell growth, migration, and proliferation.

## 6. BIOACTIVE FUNCTIONALITY CHARACTERIZATION

For *in vitro* engineered SDBVs, how to characterize the formation of bioactive endothelial layers has always been an important problem and has not been completely solved yet. Here, we will discuss several important aspects, including the markers of endothelial cells, the complete endothelial monolayer, anticoagulation, EC angiogenesis, and functional arterial-specific endothelial cells.

### 6.1. Re-Endothelialization

It has been demonstrated that the exposed luminal surface of vascular grafts may trigger thrombosis through platelet deposition. Furthermore, the delay of endothelialization and the migration and proliferation of smooth muscle cells (SMCs) may also result in intimal



hyperplasia.<sup>141</sup> Therefore, re-endothelialization is considered to be an important strategy for SDBV grafts and tissue regeneration *in vitro*. A complete endothelial monolayer ensures normal blood flow and the functional expression of ECs. For typical HUVECs, the morphology was fusiform, with a length of 30–50 microns and a width of 10–30 microns.<sup>175,176</sup> Nowadays, many methods and biomacromolecules have been developed to promote the formation of the endothelial layer on the surface of SDBV grafts.<sup>141,143,177</sup> However, how to accelerate the process of endothelialization and form a complete endothelial layer is particularly important and yet to be solved. Another key point is how to effectively inhibit the adhesion of platelets while prohibiting the adhesion, migration, and proliferation of SMCs before re-endothelialization.

## 6.2. Anticoagulation

Anticoagulation is considered to be the most important factor for long-term patency. It has been reported that platelet deposition is the major reason for thrombosis, which further results in intimal hyperplasia.<sup>178</sup> Thus, the inhibition of platelet adhesion is considered to be an ideal strategy for small-diameter vascular grafts and tissue regeneration *in vitro*.<sup>141</sup> Additionally, the activated partial thromboplastin time (APTT) and prothrombin time (PT) are blood tests that characterize the coagulation of blood and the speed of clotting, respectively. Many materials have been used to improve the anticoagulation ability, including nitric oxide (NO) and heparin.<sup>136,143,144,146</sup> Meanwhile, the anticoagulation time is another key factor. With proper coating and composites, the effective anticoagulation time can be significantly prolonged.<sup>152,178</sup> Even after re-endothelialization, the risk of endothelial cells falling off still exists, so the ability of the grafts to maintain long-term anticoagulant capacity is the ultimate goal.

## 6.3. Bioreactor

Usually, *in vitro* endothelialization is realized by bioreactors that supply biophysical and biochemical environments for cell culture.<sup>179</sup> Based on the development history of bioreactors for blood vessel applications, they can be roughly divided into three types: static, dynamic, and biomimetic bioreactors.<sup>180</sup> A static bioreactor is the most straightforward and is mainly composed of a chamber to fix scaffolds and an inlet/outlet for the introduction of medium and CO<sub>2</sub>.<sup>179</sup> One key disadvantage of a static bioreactor is non-uniform cell attachment.<sup>181</sup> To solve this issue, a lot of dynamic bioreactors have been proposed.<sup>182–184</sup> For example, rotation was allowed in Unsworth's work,<sup>183</sup> where a slow shear rate was conducive to uniform cell attachment. To better match the *in vivo* environment, more biomimetic bioreactors have been designed.<sup>185,186</sup> A simplified illustration of a biomimetic reactor is shown in Fig. 10.<sup>187</sup> Biomimetic bioreactors allow not only CO<sub>2</sub> and mass exchange, but also pulsatile circulation similar to human circulation, which simulates more *in vivo* conditions for cell proliferation and rapid endothelialization.<sup>188</sup> For the success of tissue-engineered small-diameter blood vessels, an advanced biomimetic bioreactor is necessary.

## 6.4. Arterial-Specific Functions

*In vitro*, endothelial cells (ECs) differentiated from mesenchymal stem cells are usually used for cell culture, rapid re-endothelialization, and vascular tissue regeneration and repairs.<sup>189</sup>

Characteristic genes and markers of endothelial cells—including CD31, CD34, CD144, endothelial NOS (eNOS), and von Willebrand factor (vWF)—should be detected to demonstrate the specific desired functions.<sup>190–192</sup> However, how to test the function of re-endothelialization has always been a challenge, and generating fully functional arterial endothelial cells is a critical problem for vascular development. Nowadays, the arterial-specific functions, including higher NO production, oxygen consumption, lower leukocyte adhesion, and a more sensitive response to shear stress, have been investigated by Thomson.<sup>189</sup> These are critical for modeling arterial disease *in vitro* and preventing vascular disease *in vivo*. The arterial endothelial cells were derived from human pluripotent stem cells (hPS), and the resulting xeno-free protocol produced cells with gene expression profiles, oxygen consumption rates, NO production levels, shear stress responses, and TNF $\alpha$ -induced leukocyte adhesion rates characteristic of arterial endothelial cells, as shown in Fig. 11.<sup>189</sup>

## 7. CONCLUSIONS AND PERSPECTIVES

In this review, we provided an overview of artificial SDBVs engineered *in vitro*, including material selection, manufacturing methods, surface modifications, mechanical properties, and bioactive functionalities. First, various materials—including natural polymers, synthetic polymers, tissue engineering materials, hydrogel macromolecules, and non-degradable materials—were reviewed. Natural biomaterials exhibit biocompatibility, good interaction with donor tissues, and non-toxic degradation products. However, they have quick degradation rates and their generally inferior and inconsistent mechanical properties limit the potential of a single natural material as a graft. Synthetic materials have good material consistency, suitable degradation rates, and excellent mechanical properties, which provide potential for the construction of SDBV grafts *in vitro*. However, the surface physicochemical properties of these materials affect the responsive interaction of the material with the host's extracellular matrix, and surface modification to functionalize their surfaces undoubtedly complicates the preparation process, making them less conducive to government (e.g., U.S. Food and Drug Administration, FDA) approval. Furthermore, the presence of degradation products of these materials *in vivo* and their effects on the host require further study. Non-degradable synthetic materials such as expanded polytetrafluoroethylene (ePTFE), which could serve stably *in vivo* for several years,<sup>193</sup> have been widely used in large-diameter blood vessels, thereby providing potential for SDBV clinical use. However, how to match the blood flow rate and mechanical properties of ePTFE with natural blood vessels, and how to rapidly promote endothelialization on ePTFE SDBVs, have become key issues. Thus, the combination of various materials, which may take advantage of those materials' properties, is an important research area.

Based on the material selection, various fabrication methods—including extrusion and expansion, electrospinning, thermal-induced phase separation (TIPS), braiding, 3D printing, hydrogel tubing, gas foaming, and a combination of these methods—have been used to fabricate SDBV grafts *in vitro*. The optimal combination of composite materials or processing methods to produce an artificial vessel with lifelike mechanical properties has attracted great attention. As such, suitable mechanical properties—including the modulus of elasticity, nonlinear elasticity, compliance measurement, burst pressure, and suture retention strength—are very important for preparing functional grafts. Furthermore, a variety of

surface modification methods have been developed to construct functionalized biological interfaces that contribute to improved biocompatibility, cell adhesion, anticoagulant ability, and bio-functional expression. However, complex surface modification methods are not conducive to clinical applications, so how to construct functionalized surfaces *in situ*, or construct functionalized biological scaffolds in a few simple steps, will be an important research direction.

The formation of a functionalized endothelial layer has always been an important goal. Generally, re-endothelialization is considered to be the first key point in inhibiting intimal hyperplasia and thrombosis. By using stem cells from a unique population of people who are genetically compatible donors, the wish to create artificial blood vessels that won't be rejected by a patient's body after transplantation can become a reality. As the functional arterial-specific endothelial cells fully cover the interior of the artificial blood vessel grafts and form a congruent state *in vitro*, the graft will then be transplantable. Furthermore, long-term anticoagulation ability is another important issue, contributing to the long-term patency and service of artificial blood vessels in the human body.

To date, studies on the clinical application and reaction of grafts and host are insufficient. Therefore, more attention needs to be paid to the biological response and cell culture, which will also benefit from the improvement of material selection and synthesis, fabrication, surface modification, and mechanical properties.

## ACKNOWLEDGEMENTS

The authors would like to acknowledge the support of the Wisconsin Institute for Discovery (WID) at the University of Wisconsin-Madison, the National Center for International Joint Research of Micro-Nano Molding Technology in China, the China Scholarship Council (CSC), the financial support of the International Science & Technology Cooperation Program of China (2015DFA30550), and the Key Project of Science and Technology of the Education Department of Henan Province, China (19A430003). The corresponding author at the University of Wisconsin-Madison would like to acknowledge the partial support by the NHLBI of the National Institutes of Health (grant number U01HL134655) and the Kuo K. and Cindy F. Wang Professorship.

## NOTES AND REFERENCES REFERENCES

1. Seifu DG, Purnama A, Mequanint K and Mantovani D, *Nature Reviews Cardiology*, 2013, 10, 410–421. [PubMed: 23689702]
2. L'Heureux N, Dusserre N, Marini A, Garrido S, de la Fuente L and McAllister T, *Nature Reviews Cardiology*, 2007, 4, 389–395.
3. Baker AB, *Science Translational Medicine*, 2012, 4, 144ec130–144ec130.
4. Isenberg Brett C, Williams Chrysanthi and Tranquillo Robert T, *Circulation Research*, 2006, 98, 25–35. [PubMed: 16397155]
5. Gao A, Hang R, Li W, Zhang W, Li P, Wang G, Bai L, Yu X-F, Wang H, Tong L and Chu PK, *Biomaterials*, 2017, 140, 201–211. [PubMed: 28662400]
6. Dahl SLM, Kypson AP, Lawson JH, Blum JL, Strader JT, Li Y, Manson RJ, Tente WE, DiBernardo L, Hensley MT, Carter R, Williams TP, Prichard HL, Dey MS, Begelman KG and Niklason LE, *Science Translational Medicine*, 2011, 3, 68ra9–68ra9.
7. Browning MB, Dempsey D, Guiza V, Becerra S, Rivera J, Russell B, Höök M, Clubb F, Miller M, Fossum T, Dong JF, Bergeron AL, Hahn M and Cosgriff-Hernandez E, *Acta Biomaterialia*, 2012, 8, 1010–1021. [PubMed: 22142564]
8. Ma Z, Kotaki M, Yong T, He W and Ramakrishna S, *Biomaterials*, 2005, 26, 2527–2536. [PubMed: 15585255]

9. L'Heureux N, Dusserre N, Konig G, Victor B, Keire P, Wight TN, Chronos NAF, Kyles AE, Gregory CR, Hoyt G, Robbins RC and McAllister TN, *Nature Medicine*, 2006, 12, 361–365.
10. Freed LE, Engelmayr GC, Borenstein JT, Moutos FT and Guilak F, *Advanced Materials*, 2009, 21, 3410–3418. [PubMed: 20882506]
11. Ran X, Ye Z, Fu M, Wang Q, Wu H, Lin S, Yin T, Hu T and Wang G, *Macromolecular Bioscience*, 2019, 19, 1800189.
12. de Mel A, Cousins BG and Seifalian AM, *Surface Modification of Biomaterials: A Quest for Blood Compatibility*, 2012, 707863.
13. Huang R, Gao X, Wang J, Chen H, Tong C, Tan Y and Tan Z, *Ann Biomed Eng*, 2018, 46, 1254–1266. [PubMed: 29845412]
14. Redd MA, Zeinstra N, Qin W, Wei W, Martinson A, Wang Y, Wang RK, Murry CE and Zheng Y, *Nature Communications*, 2019, 10, 584.
15. Yan S, Zhang X, Zhang L, Liu H, Wang X and Li Q, *Biomedical Materials*, 2017, 13, 015003. [PubMed: 29125131]
16. Cui H, Zhu W, Holmes B and Zhang LG, *Advanced Science*, 2016, 3, 1600058–1600067. [PubMed: 27818910]
17. Weidenbacher L, Müller E, Guex AG, Zündel M, Schweizer P, Marina V, Adlhart C, Vejsadová L, Pauer R, Spiecker E, Maniura-Weber K, Ferguson SJ, Rossi RM, Rottmar M and Fortunato G, *ACS Appl. Mater. Interfaces*, 2019, 11, 5740–5751. [PubMed: 30668107]
18. Radke D, Jia W, Sharma D, Fena K, Wang G, Goldman J and Zhao F, *Advanced Healthcare Materials*, 2018, 7, 1701461.
19. Carrabba M and Madeddu P, *Front Bioeng Biotechnol*, 2018, 6, 41. [PubMed: 29721495]
20. Zou Y, Zhang L, Yang L, Zhu F, Ding M, Lin F, Wang Z and Li Y, *Journal of Controlled Release*, 2018, 273, 160–179. [PubMed: 29382547]
21. Weinberg CB and Bell E, *Science*, 1986, 231, 397–400. [PubMed: 2934816]
22. Devalliere J, Chen Y, Dooley K, Yarmush ML and Uygun BE, *Acta Biomaterialia*, 2018, 78, 151–164. [PubMed: 30071351]
23. Liao S, He Q, Yang L, Liu S, Zhang Z, Guidoin R, Fu Q and Xie X, *Journal of Biomedical Materials Research Part B: Applied Biomaterials*, 2019, 107, 965–977. [PubMed: 30265778]
24. Malafaya PB, Silva GA and Reis RL, *Advanced Drug Delivery Reviews*, 2007, 59, 207–233. [PubMed: 17482309]
25. Zhang H, Jia X, Han F, Zhao J, Zhao Y, Fan Y and Yuan X, *Biomaterials*, 2013, 34, 2202–2212. [PubMed: 23290468]
26. Li Y, Jiang K, Feng J, Liu J, Huang R, Chen Z, Yang J, Dai Z, Chen Y, Wang N, Zhang W, Zheng W, Yang G and Jiang X, *Advanced Healthcare Materials*, 2017, 6, 1601343.
27. Yoon DM and Fisher JP, in *Biomedical Materials*, ed. Narayan R, Springer US, Boston, MA, 2009, pp. 415–442.
28. Sell SA, Wolfe PS, Garg K, McCool JM, Rodriguez IA and Bowlin GL, *Polymers*; Basel, 2010, 2, 522–553.
29. Huynh T, Abraham G, Murray J, Brockbank K, Hagen P-O and Sullivan S, *Nature Biotechnology*, 1999, 17, 1083.
30. Jiang Y-C, Wang X-F, Xu Y-Y, Qiao Y-H, Guo X, Wang D-F, Li Q and Turng L-S, *Biomacromolecules*, 2018, 19, 3747–3753. [PubMed: 30095899]
31. Koens MJW, Faraj KA, Wismans RG, van der Vliet JA, Krasznai AG, Cuijpers VMJI, Jansen JA, Daamen WF and van Kuppevelt TH, *Acta Biomaterialia*, 2010, 6, 4666–4674. [PubMed: 20619367]
32. Li C, Vepari C, Jin H-J, Kim HJ and Kaplan DL, *Biomaterials*, 2006, 27, 3115–3124. [PubMed: 16458961]
33. Bergmeister H, Seyidova N, Schreiber C, Strobl M, Grasl C, Walter I, Messner B, Baudis S, Fröhlich S, Marchetti-Deschmann M, Griesser M, di Franco M, Krssak M, Liska R and Schima H, *Acta Biomaterialia*, 2015, 11, 104–113. [PubMed: 25218664]
34. Brown EE, Hu D, Abu Lail N and Zhang X, *Biomacromolecules*, 2013, 14, 1063–1071. [PubMed: 23421631]

35. Tillman BW, Yazdani SK, Lee SJ, Geary RL, Atala A and Yoo JJ, *Biomaterials*, 2009, 30, 583–588. [PubMed: 18990437]
36. Lu J, Zhuang W, Li L, Zhang B, Yang L, Liu D, Yu H, Luo R and Wang Y, *ACS Appl. Mater. Interfaces*, 2019, 11, 10337–10350. [PubMed: 30753784]
37. Zhang J, Wang D, Jiang X, He L, Fu L, Zhao Y, Wang Y, Mo H and Shen J, *Chemical Engineering Journal*, 2019, 370, 1057–1067.
38. Detta N, Errico C, Dinucci D, Puppi D, Clarke DA, Reilly GC and Chiellini F, *J Mater Sci: Mater Med*, 2010, 21, 1761–1769. [PubMed: 20135202]
39. Saroia J, Yanen W, Wei Q, Zhang K, Lu T and Zhang B, *Bio-des. Manuf*, 2018, 1, 265–279.
40. Liu H, Zhou H, Lan H, Liu T, Liu X and Yu H, *Micromachines*, 2017, 8, 237.
41. Marelli B, Alessandrino A, Farè S, Freddi G, Mantovani D and Tanzi MC, *Acta Biomaterialia*, 2010, 6, 4019–4026. [PubMed: 20466080]
42. Zhang Y, Li XS, Guex AG, Liu SS, Müller E, Malini RI, Zhao HJ, Rottmar M, Maniura-Weber K, Rossi RM and Spano F, *Biofabrication*, 2017, 9, 025010. [PubMed: 28382923]
43. Mi H-Y, Jiang Y, Jing X, Enriquez E, Li H, Li Q and Turng L-S, *Materials Science and Engineering: C*, 2019, 98, 241–249. [PubMed: 30813024]
44. Yue K, Trujillo-de Santiago G, Alvarez MM, Tamayol A, Annabi N and Khademhosseini A, *Biomaterials*, 2015, 73, 254–271. [PubMed: 26414409]
45. Zhao Q, Wang J, Cui H, Chen H, Wang Y and Du X, *Advanced Functional Materials*, 2018, 1801027.
46. Mo X, Weber H-J and Ramakrishna S, *The International Journal of Artificial Organs*, 2006, 29, 790–799. [PubMed: 16969757]
47. Hu X, Shen H, Yang F, Bei J and Wang S, *Biomaterials*, 2008, 29, 3128–3136. [PubMed: 18439673]
48. Ku SH and Park CB, *Biomaterials*, 2010, 31, 9431–9437. [PubMed: 20880578]
49. Lee SJ, Liu J, Oh SH, Soker S, Atala A and Yoo JJ, *Biomaterials*, 2008, 29, 2891–2898. [PubMed: 18400292]
50. Tang D, Chen S, Hou D, Gao J, Jiang L, Shi J, Liang Q, Kong D and Wang S, *Materials Science and Engineering: C*, 2018, 84, 1–11. [PubMed: 29519417]
51. Zhang M, Li XH, Gong YD, Zhao NM and Zhang XF, *Biomaterials*, 2002, 23, 2641–2648. [PubMed: 12059013]
52. Lee K-W, Johnson NR, Gao J and Wang Y, *Biomaterials*, 2013, 34, 9877–9885. [PubMed: 24060423]
53. Loh XJ, Karim AA and Owh C, *J. Mater. Chem. B*, 2015, 3, 7641–7652. [PubMed: 32264574]
54. Niklason LE, Gao J, Abbott WM, Hirschi KK, Houser S, Marini R and Langer R, *Science*, 1999, 284, 489–493. [PubMed: 10205057]
55. Li C, Wang F, Douglas G, Zhang Z, Guidoin R and Wang L, *Journal of the Mechanical Behavior of Biomedical Materials*, 2017, 69, 39–49. [PubMed: 28038405]
56. Li L-Y, Cui L-Y, Zeng R-C, Li S-Q, Chen X-B, Zheng Y and Kannan MB, *Acta Biomaterialia*, 2018, 79, 23–36. [PubMed: 30149212]
57. Kabinejadian F and Ghista DN, *Medical Engineering & Physics*, 2012, 34, 860–872. [PubMed: 22032834]
58. Catto V, Farè S, Freddi G and Tanzi MC, *Vascular Medicine*, 2014, 923930.
59. Pu FR, Williams RL, Markkula TK and Hunt JA, *Biomaterials*, 2002, 23, 4705–4718. [PubMed: 12361609]
60. Walluscheck KP, Steinhoff G, Kelm S and Haverich A, *European Journal of Vascular and Endovascular Surgery*, 1996, 12, 321–330. [PubMed: 8896475]
61. Khan MQ, Kharaghani D, Nishat N, Sanaullah A, Shahzad, Yamamoto T, Inoue Y and Kim IS, *Journal of Applied Polymer Science*, 2019, 136, 47222.
62. Hutmacher DW, *Journal of Biomaterials Science, Polymer Edition*, 2001, 12, 107–124. [PubMed: 11334185]
63. Hench LL and Polak JM, *Science*, 2002, 295, 1014–1017. [PubMed: 11834817]

64. Kumar VA, Brewster LP, Caves JM and Chaikof EL, *Cardiovasc Eng Technol*, 2011, 2, 137–148. [PubMed: 23181145]
65. Elbaz A, He Z, Gao B, Chi J, Su E, Zhang D, Liu S, Xu H, Liu H and Gu Z, *Bio-des. Manuf*, 2018, 1, 26–44.
66. Soletti L, Hong Y, Guan J, Stankus JJ, El-Kurdi MS, Wagner WR and Vorp DA, *Acta Biomaterialia*, 2010, 6, 110–122. [PubMed: 19540370]
67. Rajangam K, Behanna HA, Hui MJ, Han X, Hulvat JF, Lomasney JW and Stupp SI, *Nano Lett*, 2006, 6, 2086–2090. [PubMed: 16968030]
68. Zhang WJ, Liu W, Cui L and Cao Y, *Journal of Cellular and Molecular Medicine*, 2007, 11, 945–957. [PubMed: 17979876]
69. A tough biodegradable elastomer | *Nature Biotechnology*, <https://www.nature.com/articles/nbt0602-602>, (accessed December 26, 2019).
70. Ji W, Yang F, Seyednejad H, Chen Z, Hennink WE, Anderson JM, van den Beucken JJJP and Jansen JA, *Biomaterials*, 2012, 33, 6604–6614. [PubMed: 22770568]
71. Lam CXF, Savalani MM, Teoh S-H and Hutmacher DW, *Biomed. Mater*, 2008, 3, 034108. [PubMed: 18689929]
72. Rodenas-Rochina J, Vidaurre A, Castilla Cortázar I and Lebourg M, *Polymer Degradation and Stability*, 2015, 119, 121–131.
73. Chu CC, *Journal of Applied Polymer Science*, 1981, 26, 1727–1734.
74. Wang Y, Kim YM and Langer R, *Journal of Biomedical Materials Research Part A*, 2003, 66A, 192–197.
75. Damink LHHO, Dijkstra PJ, van Luyn MJA, van Wachem PB, Nieuwenhuis P and Feijen J, *Biomaterials*, 1996, 17, 679–684. [PubMed: 8672629]
76. Shum AWT and Mak AFT, *Polymer Degradation and Stability*, 2003, 81, 141–149.
77. Harrane A, Leroy A, Nouailhas H, Garric X, Coudane J and Nottelet B, *Biomed. Mater*, 2011, 6, 065006. [PubMed: 22101003]
78. Husmann M, Schenderlein S, Lück M, Lindner H and Kleinebudde P, *International Journal of Pharmaceutics*, 2002, 242, 277–280. [PubMed: 12176263]
79. Gonzalez MF, Ruseckaite RA and Cuadrado TR, *Journal of Applied Polymer Science*, 1999, 71, 1223–1230.
80. Tatai L, Moore TG, Adhikari R, Malherbe F, Jayasekara R, Griffiths I and Gunatillake PA, *Biomaterials*, 2007, 28, 5407–5417. [PubMed: 17915310]
81. Koski A, Yim K and Shivkumar S, *Materials Letters*, 2004, 58, 493–497.
82. Ansari M and Eshghanmalek M, *Bio-des. Manuf*, 2019, 2, 41–49.
83. Ying G, Jiang N, Yu C and Zhang YS, *Bio-des. Manuf*, 2018, 1, 215–224.
84. Xue L and Greisler HP, *Journal of Vascular Surgery*, 2003, 37, 472–480. [PubMed: 12563226]
85. Walpoth BH and Bowlin GL, *Expert Review of Medical Devices*, 2005, 2, 647–651. [PubMed: 16293089]
86. Sullivan SJ, Maki T, Borland KM, Mahoney MD, Solomon BA, Muller TE, Monaco AP and Chick WL, *Science*, 1991, 252, 718–721. [PubMed: 2024124]
87. Hess F, *Microsurgery*, 1985, 6, 59–69. [PubMed: 3894875]
88. Damme HV, Deprez M, Creemers E and Limet R, *Acta Chirurgica Belgica*, 2005, 105, 249–255. [PubMed: 16018516]
89. Geelhoed WJ, Moroni L and Rotmans JI, *J Cardiovasc Transl Res*, 2017, 10, 167–179. [PubMed: 28205013]
90. Ranjbarzadeh-Dibazar A, Barzin J and Shokrollahi P, *Polymer*, 2017, 121, 75–87.
91. Ranjbarzadeh-Dibazar A, Shokrollahi P, Barzin J and Rahimi A, *Journal of Membrane Science*, 2014, 470, 458–469.
92. Hoshi RA, Van Lith R, Jen MC, Allen JB, Lapidos KA and Ameer G, *Biomaterials*, 2013, 34, 30–41. [PubMed: 23069711]
93. United States, US3953556A, 1976.
94. United States, US3664906A, 1972.

95. Huang Q, Xiao C and Hu X, *J Mater Sci*, 2010, 45, 6569–6573.
96. Ainslie KM, Bachelder EM, Borkar S, Zahr AS, Sen A, Badding JV and Pishko MV, *Langmuir*, 2007, 23, 747–754. [PubMed: 17209629]
97. Wang F, Li J, Zhu H, Zhang H, Tang H, Chen J and Guo Y, *Journal of Water Process Engineering*, 2015, 7, 36–45.
98. Zilla P, Bezuidenhout D and Human P, *Biomaterials*, 2007, 28, 5009–5027. [PubMed: 17688939]
99. Golden MA, Hanson SR, Kirkman TR, Schneider PA and Clowes AW, *Journal of Vascular Surgery*, 1990, 11, 838–845. [PubMed: 2359196]
100. Doshi J and Reneker DH, *Journal of Electrostatics*, 1995, 35, 151–160.
101. Ashraf R, Sofi HS, Malik A, Beigh MA, Hamid R and Sheikh FA, *Appl Biochem Biotechnol*, 2019, 187, 47–74. [PubMed: 29882194]
102. Teo WE and Ramakrishna S, *Nanotechnology*, 2006, 17, R89–R106. [PubMed: 19661572]
103. Pham QP, Sharma U and Mikos AG, *Tissue Engineering*, 2006, 12, 1197–1211. [PubMed: 16771634]
104. Goonoo N, *Advanced Biosystems*, 2017, 1, 1700093.
105. Geng X, Kwon O-H and Jang J, *Biomaterials*, 2005, 26, 5427–5432. [PubMed: 15860199]
106. Mi H-Y, Jing X and Turng L-S, *Journal of Cellular Plastics*, 2015, 51, 165–196.
107. Casper CL, Stephens JS, Tassi NG, Chase DB and Rabolt JF, *Macromolecules*, 2004, 37, 573–578.
108. Jiang H, Hu Y, Li Y, Zhao P, Zhu K and Chen W, *Journal of Controlled Release*, 2005, 108, 237–243. [PubMed: 16153737]
109. Yu E, Mi H-Y, Zhang J, Thomson JA and Turng L-S, *Journal of Biomedical Materials Research Part A*, 2018, 106, 985–996. [PubMed: 29143442]
110. Liu K, Wang N, Wang W, Shi L, Li H, Guo F, Zhang L, Kong L, Wang S and Zhao Y, *J. Mater. Chem. B*, 2017, 5, 3758–3764. [PubMed: 32264064]
111. Wu T, Zhang J, Wang Y, Li D, Sun B, El-Hamshary H, Yin M and Mo X, *Materials Science and Engineering: C*, 2018, 82, 121–129. [PubMed: 29025640]
112. Kuang H, Wang Y, Hu J, Wang C, Lu S and Mo X, *ACS Applied Materials & Interfaces*, 2018, 10, 19365–19372. [PubMed: 29782791]
113. Lo H, Ponticciello M. s. and Leong K. w., *Tissue Engineering*, 1995, 1, 15–28. [PubMed: 19877912]
114. Ma H, Hu J and Ma PX, *Adv Funct Mater*, 2010, 20, 2833–2841. [PubMed: 24501590]
115. Yu Q, Sun Z, Qiu Y, Zhou S, Chen Y, Wu J, Zhou Q and Chen X, *Textile Research Journal*, 2019, 89, 172–181.
116. Al Meslmani BM, Mahmoud GF and Bakowsky U, *Journal of Drug Delivery Science and Technology*, 2018, 47, 144–150.
117. Kudo FA, Nishibe T, Miyazaki K, Flores J and Yasuda K, *International angiology : a journal of the International Union of Angiology*, 2002, 21, 214–217. [PubMed: 12384639]
118. Singh C, Wong CS and Wang X, *Journal of Functional Biomaterials; Basel*, 2015, 6, 500–525.
119. Nakazawa Y, Sato M, Takahashi R, Aytemiz D, Takabayashi C, Tamura T, Enomoto S, Sata M and Asakura T, *Journal of Biomaterials Science, Polymer Edition*, 2011, 22, 195–206. [PubMed: 20557695]
120. Radenkovic D, Solouk A and Seifalian A, *Medical Hypotheses*, 2016, 87, 30–33. [PubMed: 26826637]
121. Holland I, Logan J, Shi J, McCormick C, Liu D and Shu W, *Bio-des. Manuf*, 2018, 1, 89–100.
122. Melchiorri AJ, Hibino N, Best CA, Yi T, Lee YU, Kraynak CA, Kimerer LK, Krieger A, Kim P, Breuer CK and Fisher JP, *Advanced Healthcare Materials*, 2016, 5, 319–325. [PubMed: 26627057]
123. Mosadegh B, Xiong G, Dunham S and Min JK, *Biomed. Mater*, 2015, 10, 034002. [PubMed: 25775166]
124. Deng J, Cheng C, Teng Y, Nie C and Zhao C, *Polym. Chem*, 2017, 8, 2266–2275.

125. Alexandre N, Costa E, Coimbra S, Silva A, Lopes A, Rodrigues M, Santos M, Maurício AC, Santos JD and Luís AL, *Journal of Biomedical Materials Research Part A*, 2015, 103, 1366–1379. [PubMed: 25044790]
126. Thein-Han W and Xu HHK, *Tissue Engineering Part A*, 2013, 19, 1675–1685. [PubMed: 23470207]
127. Sun S, Li Q, Zhao N, Jiang J, Zhang K, Hou J, Wang X and Liu G, *Polymers for Advanced Technologies*, 2018, 29, 3065–3074.
128. Lv Z, Zhao N, Wu Z, Zhu C and Li Q, *Ind. Eng. Chem. Res.*, 2018, 57, 12951–12958.
129. Mi H-Y, Jing X, Yu E, McNulty J, Peng X-F and Turng L-S, *Materials Letters*, 2015, 161, 305–308.
130. Jin Lee S, Nyoung Heo D, Sun Park J, Keun Kwon S, Ho Lee J, Hee Lee J, Doo Kim W, Keun Kwon I and Park SA, *Physical Chemistry Chemical Physics*, 2015, 17, 2996–2999. [PubMed: 25557615]
131. Song J, Zhu G, Gao H, Wang L, Li N, Shi X and Wang Y, *Bio-des. Manuf*, 2018, 1, 254–264.
132. Chung HJ and Park TG, *Advanced Drug Delivery Reviews*, 2007, 59, 249–262. [PubMed: 17482310]
133. Wang D, Wang X, Li X, Jiang L, Chang Z and Li Q, *Materials Science and Engineering: C*, 2020, 107, 110212. [PubMed: 31761208]
134. Yoo HS, Kim TG and Park TG, *Advanced Drug Delivery Reviews*, 2009, 61, 1033–1042. [PubMed: 19643152]
135. Mi H-Y, Jing X, Thomsom JA and Turng L-S, *J. Mater. Chem. B*, 2018, 6, 3475–3485. [PubMed: 30455952]
136. Zhu AP, Ming Z and Jian S, *Applied Surface Science*, 2005, 241, 485–492.
137. Lee YB, Shin YM, Lee J, Jun I, Kang JK, Park J-C and Shin H, *Biomaterials*, 2012, 33, 8343–8352. [PubMed: 22917738]
138. Lee H, Dellatore SM, Miller WM and Messersmith PB, *Science*, 2007, 318, 426–430. [PubMed: 17947576]
139. Mi H-Y, Jing X, Li Z-T, Lin Y-J, Thomson JA and Turng L-S, *Journal of Biomedical Materials Research Part B: Applied Biomaterials*, 2019, b.34333.
140. He C, Ji H, Qian Y, Wang Q, Liu X, Zhao W and Zhao C, *J. Mater. Chem. B*, 2019, 7, 1186–1208. [PubMed: 32255159]
141. Wang Y, Chen S, Pan Y, Gao J, Tang D, Kong D and Wang S, *Journal of Materials Chemistry B*, 2015, 3, 9212–9222. [PubMed: 32263136]
142. Chiu LLY and Radisic M, *Biomaterials*, 2010, 31, 226–241. [PubMed: 19800684]
143. Yang Z, Yang Y, Xiong K, Li X, Qi P, Tu Q, Jing F, Weng Y, Wang J and Huang N, *Biomaterials*, 2015, 63, 80–92. [PubMed: 26093790]
144. Yang Z, Yang Y, Zhang L, Xiong K, Li X, Zhang F, Wang J, Zhao X and Huang N, *Biomaterials*, 2018, 178, 1–10. [PubMed: 29902532]
145. Wang D, Xu Y, Wang L, Wang X, Yan S, Yilmaz G, Li Q and Turng L-S, *Applied Surface Science*, 2020, 507, 145028.
146. Zhang F, Zhang Q, Li X, Huang N, Zhao X and Yang Z, *Biomaterials*, 2019, 194, 117–129. [PubMed: 30590241]
147. Wang D, Wang X, Zhang Z, Wang L, Li X, Xu Y, Ren C, Li Q and Turng L-S, *ACS Appl. Mater. Interfaces*, 2019, 11, 32533–32542. [PubMed: 31393107]
148. Rivron NC, Vrij EJ, Rouwkema J, Gac SL, van den Berg A, Truckenmüller RK and van Blitterswijk CA, *PNAS*, 2012, 109, 6886–6891. [PubMed: 22511716]
149. Wang P, Xiong P, Liu J, Gao S, Xi T and Cheng Y, *J. Mater. Chem. B*, 2018, 6, 966–978. [PubMed: 32254377]
150. Mao C, Qiu Y, Sang H, Mei H, Zhu A, Shen J and Lin S, *Advances in Colloid and Interface Science*, 2004, 110, 5–17. [PubMed: 15142821]
151. Keeney M, Jiang XY, Yamane M, Lee M, Goodman S and Yang F, *J. Mater. Chem. B*, 2015, 3, 8757–8770. [PubMed: 27099754]



152. Du H, Tao L, Wang W, Liu D, Zhang Q, Sun P, Yang S and He C, *Materials Science and Engineering: C*, 2019, 100, 845–854. [PubMed: 30948122]
153. Gao J, Jiang L, Liang Q, Shi J, Hou D, Tang D, Chen S, Kong D and Wang S, *Regen Biomater*, 2018, 5, 105–114. [PubMed: 29644092]
154. Ye J, Si J, Cui Z, Wang Q, Peng K, Chen W, Peng X and Chen S-C, *Macromolecular Materials and Engineering*, 2017, 302, 1700277.
155. Kleinhans C, Barz J, Wurster S, Willig M, Oehr C, Müller M, Walles H, Hirth T and Kluger PJ, *Biotechnology Journal*, 2013, 8, 327–337. [PubMed: 23070995]
156. van Kooten TG, Spijker HT and Busscher HJ, *Biomaterials*, 2004, 25, 1735–1747. [PubMed: 14738836]
157. Bax DV, Wang Y, Li Z, Maitz PKM, McKenzie DR, Bilek MMM and Weiss AS, *Biomaterials*, 2011, 32, 5100–5111. [PubMed: 21527206]
158. Shin YM, Lee YB, Kim SJ, Kang JK, Park J-C, Jang W and Shin H, *Biomacromolecules*, 2012, 13, 2020–2028. [PubMed: 22617001]
159. Hamedani BA, Navidbakhsh M and Tafti HA, *BioMedical Engineering OnLine*, 2012, 11, 59. [PubMed: 22917177]
160. Holzapfel GA, Sommer G, Gasser CT and Regitnig P, *American Journal of Physiology-Heart and Circulatory Physiology*, 2005, 289, H2048–H2058. [PubMed: 16006541]
161. van Andel CJ, Pistecky PV and Borst C, *The Annals of Thoracic Surgery*, 2003, 76, 58–64. [PubMed: 12842513]
162. Roeder R, Wolfe J, Lianakis N, Hinson T, Geddes LA and Obermiller J, *Journal of Biomedical Materials Research*, 1999, 47, 65–70. [PubMed: 10400882]
163. Abdal-hay A, Bartnikowski M, Hamlet S and Ivanovski S, *Materials Science and Engineering: C*, 2018, 82, 10–18. [PubMed: 29025637]
164. Boron WF and Boulpaep EL, *Medical Physiology E-Book*, Elsevier Health Sciences, 2016.
165. Niu Z, Wang X, Meng X, Guo X, Jiang Y, Xu Y, Li Q and Shen C, *Biomed. Mater*, 2019, 14, 035006. [PubMed: 30776786]
166. de Valence S, Tille J-C, Mugnai D, Mrowczynski W, Gurny R, Möller M and Walpoth BH, *Biomaterials*, 2012, 33, 38–47. [PubMed: 21940044]
167. Sonoda H, Takamizawa K, Nakayama Y, Yasui H and Matsuda T, *Journal of Biomedical Materials Research*, 2001, 55, 266–276. [PubMed: 11255179]
168. Sarkar S, Salacinski HJ, Hamilton G and Seifalian AM, *European Journal of Vascular and Endovascular Surgery*, 2006, 31, 627–636. [PubMed: 16513376]
169. Stewart SFC and Lyman DJ, *Journal of Biomechanics*, 1992, 25, 297–310. [PubMed: 1564063]
170. König G, McAllister TN, Dusserre N, Garrido SA, Iyican C, Marini A, Fiorillo A, Avila H, Wystrychowski W, Zagalski K, Maruszewski M, Jones AL, Cierpka L, de la Fuente LM and L'Heureux N, *Biomaterials*, 2009, 30, 1542–1550. [PubMed: 19111338]
171. Li C, Wang F, Douglas G, Zhang Z, Guidoin R and Wang L, *Journal of the Mechanical Behavior of Biomedical Materials*, 2017, 69, 39–49. [PubMed: 28038405]
172. Zhu M, Wu Y, Li W, Dong X, Chang H, Wang K, Wu P, Zhang J, Fan G, Wang L, Liu J, Wang H and Kong D, *Biomaterials*, 2018, 183, 306–318. [PubMed: 30189358]
173. Drilling S, Gaumer J and Lannutti J, *Journal of Biomedical Materials Research Part A*, 2009, 88A, 923–934.
174. Chaparro FJ, Matusicky ME, Allen MJ and Lannutti JJ, *Journal of Biomedical Materials Research Part B: Applied Biomaterials*, 2016, 104, 1525–1534. [PubMed: 26256447]
175. Boshoff C, Schulz TF, Kennedy MM, Graham AK, Fisher C, Thomas A, McGee JO, Weiss RA and O'Leary JJ, *Nature Medicine*, 1995, 1, 1274.
176. Onoe H, Okitsu T, Itou A, Kato-Negishi M, Gojo R, Kiriya D, Sato K, Miura S, Iwanaga S, Kuribayashi-Shigetomi K, Matsunaga YT, Shimoyama Y and Takeuchi S, *Nature Materials*, 2013, 12, 584–590. [PubMed: 23542870]
177. Farkas L, Beiske K, Lund-Johansen F, Brandtzaeg P and Jahnsen FL, *The American Journal of Pathology*, 2001, 159, 237–243. [PubMed: 11438470]

178. Zheng W, Wang Z, Song L, Zhao Q, Zhang J, Li D, Wang S, Han J, Zheng X-L, Yang Z and Kong D, *Biomaterials*, 2012, 33, 2880–2891. [PubMed: 22244694]
179. FREED L, *Principle of Tissue Engineering USA*, 2000, 143–156.
180. Barron V, Lyons E, Stenson-Cox C, McHugh PE and Pandit A, *Annals of Biomedical Engineering*, 2003, 31, 1017–1030. [PubMed: 14582605]
181. Freed LE and Vunjak-Novakovic G, CA: Academic, 2002, 97–110.
182. Sutherland FWH, Perry TE, Nasser BA, Wang J, Kaushal S, Guleserian KJ, Martin DP, Vacant JP and Mayer JEJ, *ASAIO Journal*, 2002, 48, 346. [PubMed: 12141461]
183. Unsworth BR and Lelkes PI, *Nat Med*, 1998, 4, 901–907. [PubMed: 9701241]
184. *Microgravity Studies of Cells and Tissues - VUNJAK-NOVAKOVIC - 2002 - Annals of the New York Academy of Sciences - Wiley Online Library*, <https://nyaspubs.onlinelibrary.wiley.com/doi/abs/10.1111/j.1749-6632.2002.tb05927.x>, (accessed December 26, 2019).
185. *New Pulsatile Bioreactor for In Vitro Formation of Tissue Engineered Heart Valves | Tissue Engineering*, <https://www.liebertpub.com/doi/abs/10.1089/107632700320919>, (accessed December 26, 2019).
186. Hoerstrup SP, Zünd G, Sodian R, Schnell AM, Grünenfelder J and Turina MI, *Eur J Cardiothorac Surg*, 2001, 20, 164–169. [PubMed: 11423291]
187. Seliktar D, Black RA, Vito RP and Nerem RM, *Annals of Biomedical Engineering*, 2000, 28, 351–362. [PubMed: 10870892]
188. Niklason LE and Langer RS, *Transplant Immunology*, 1997, 5, 303–306. [PubMed: 9504152]
189. Zhang J, Chu L-F, Hou Z, Schwartz MP, Hacker T, Vickerman V, Swanson S, Leng N, Nguyen BK, Elwell A, Bolin J, Brown ME, Stewart R, Burlingham WJ, Murphy WL and Thomson JA, *Proceedings of the National Academy of Sciences*, 2017, 114, E6072–E6078.
190. Yanagisawa M, Kurihara H, Kimura S, Tomobe Y, Kobayashi M, Mitsui Y, Yazaki Y, Goto K and Masaki T, *Nature*, 1988, 332, 411. [PubMed: 2451132]
191. Plein A, Fantin A, Denti L, Pollard JW and Ruhrberg C, *Nature*, 2018, 562, 223. [PubMed: 30258231]
192. Furchgott RF and Zawadzki JV, *Nature*, 1980, 288, 373. [PubMed: 6253831]
193. *Eight years of clinical endothelial cell transplantation. Closing the gap between prosthetic grafts and vein grafts. - Abstract - Europe PMC*, <https://europepmc.org/article/med/9360096>, (accessed December 26, 2019).



**Fig. 1.** The five pillars of artificial small-diameter blood vessels (SDBVs) engineered *in vitro*.

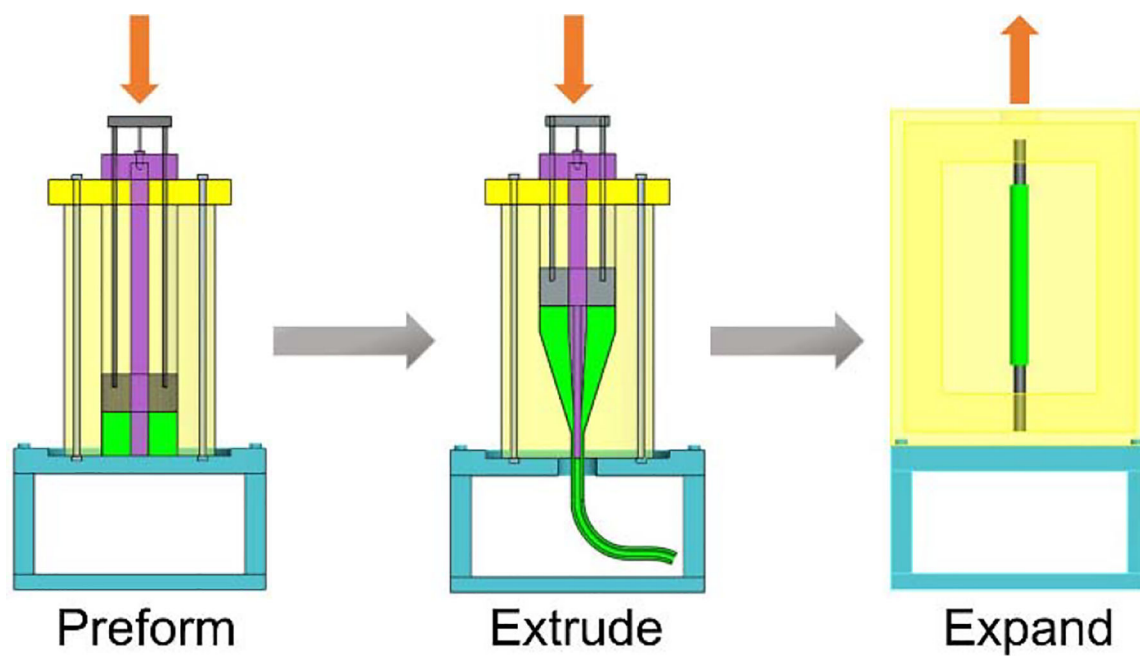


**Fig. 2.**  
The techniques of manufacturing ePTFE by means of mixing, extruding, heating, and stretching.

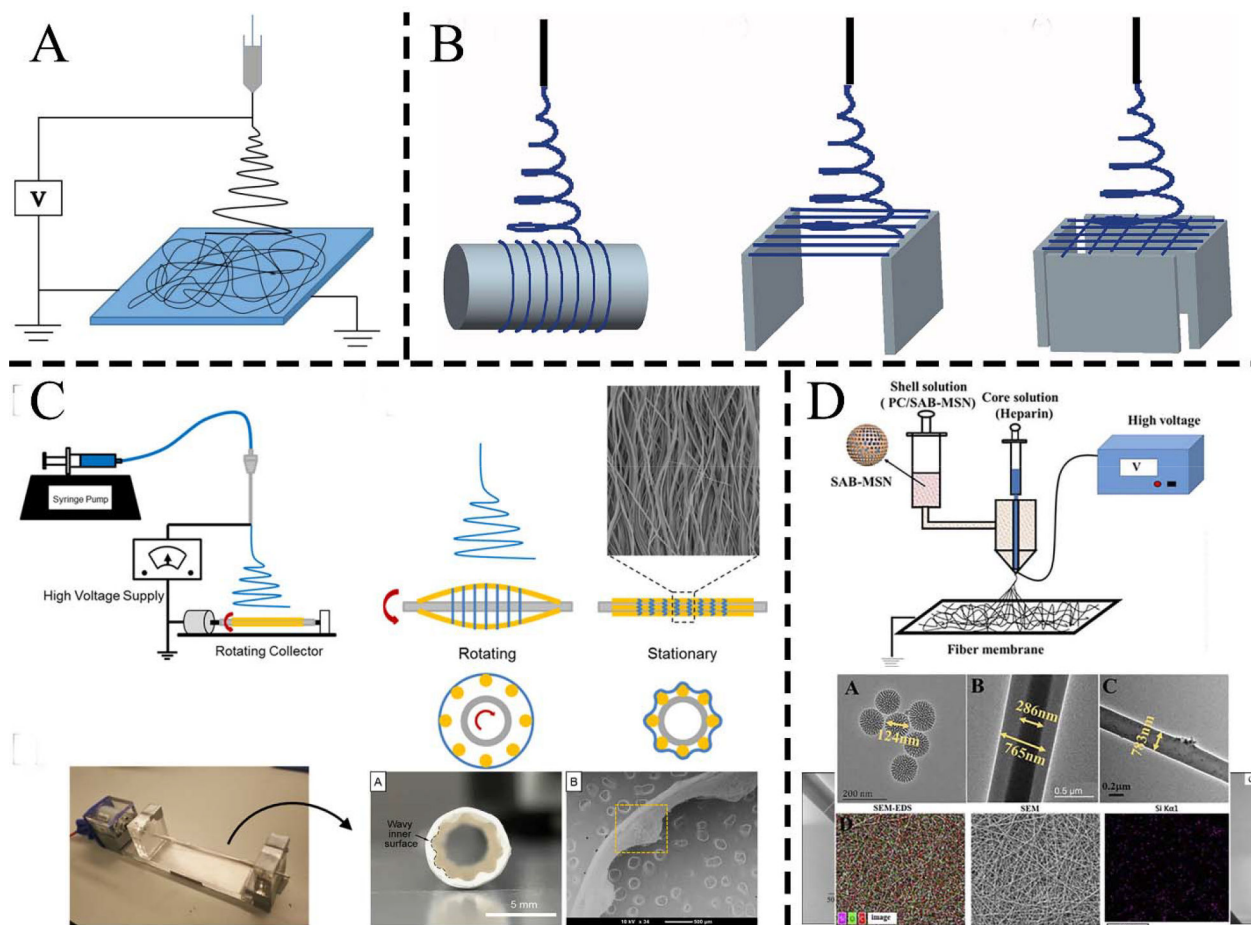


**Fig. 3.** (A) Schematic illustration of the electrospinning setup. (B) Schematic illustration of traditional electrospinning collection devices for the fabrication of tissue scaffolds with specific fiber orientations. (C) Schematic of the electrospinning apparatus with a customized rotating collector and assembled mandrel. The assembled mandrel is comprised of a hollow metal tube at the center and several surrounding satellite cylinders for making wavy SDBVs. (D) Coaxial electrospinning. (B–D) were reprinted with permission from Ref. 106: Copyright (2015) SAGE journals, Ref. 109: Copyright (2018) Wiley Online Library, and Ref. 112: Copyright (2018) ACS Publications, respectively.

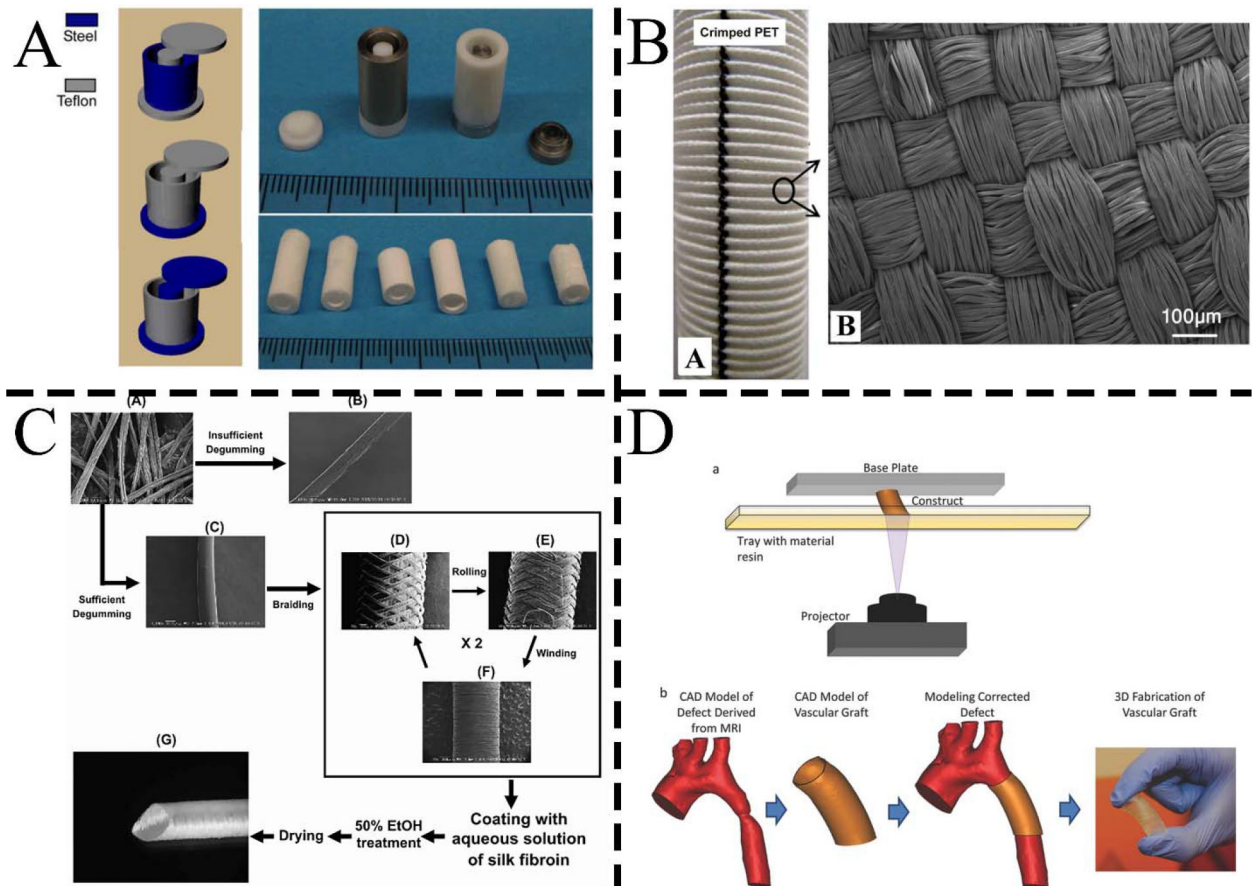


**Fig. 4.** (A) Schematic illustration of the molds for preparing oriented gradient microtubule-structured scaffolds by TIPS. (B) The image of the woven form of the crimped multifilament polyethylene terephthalate (PET) graft fabricated in an over-and-under pattern. (C) The preparation process of silk fibers and silk grafts at several processing stages, including raw silk, degumming, removal of silk sericin, braiding, rolling, and silk graft after winding. (D) The resin was printed by microlithography for SDBVs. (A–D) were reprinted with permission from Ref. 114: Copyright (2010) Wiley Online Library, Ref. 116: Copyright (2018) Elsevier, Ref. 119: Copyright (2011) Taylor & Francis Online, and Ref. 122. Copyright (2016): Wiley Online Library, respectively.

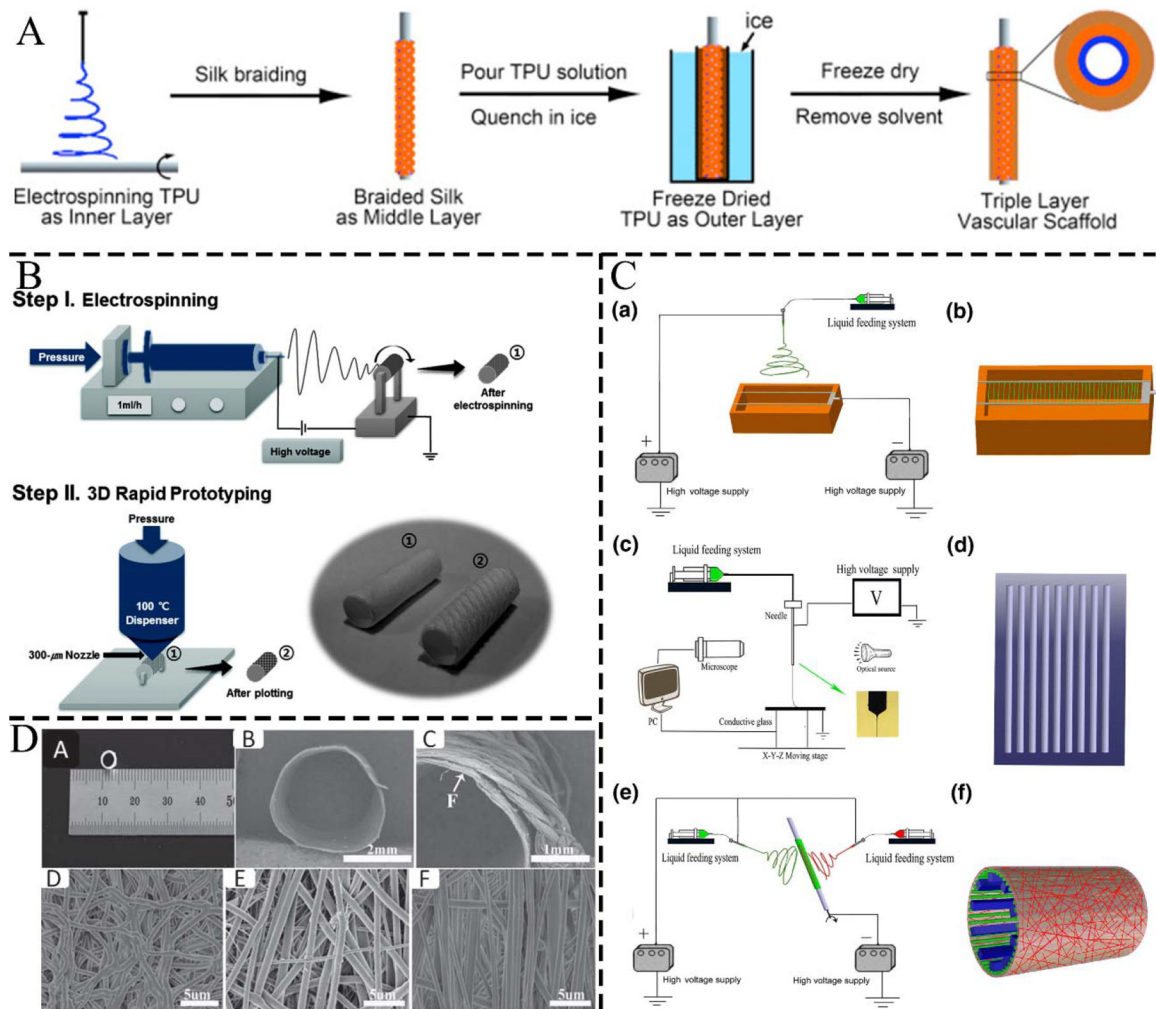


**Fig. 5.** (A) Schematic illustration of fabricating triple-layered vascular scaffolds by combining electrospinning, braiding, and thermally induced phase separation (TIPS). (B) Schematic illustration of fabricating 3D tubular artificial vascular scaffolds by combining electrospinning and a 3D printing system. (C) A compliant and biomimetic three-layered vascular graft for small blood vessels by combining electrospinning and braiding. (D) The fabrication process of triple-layered vascular grafts by combined e-Jet 3D printing and electrospinning. (A–D) were reprinted/reproduced with permission from Ref. 129: Copyright (2015) Elsevier, Ref. 130: Copyright (2015) Royal Society of Chemistry, Ref. 13: Copyright (2018) Springer, and Ref. 42: Copyright (2019) IOPSCIENCE, respectively.

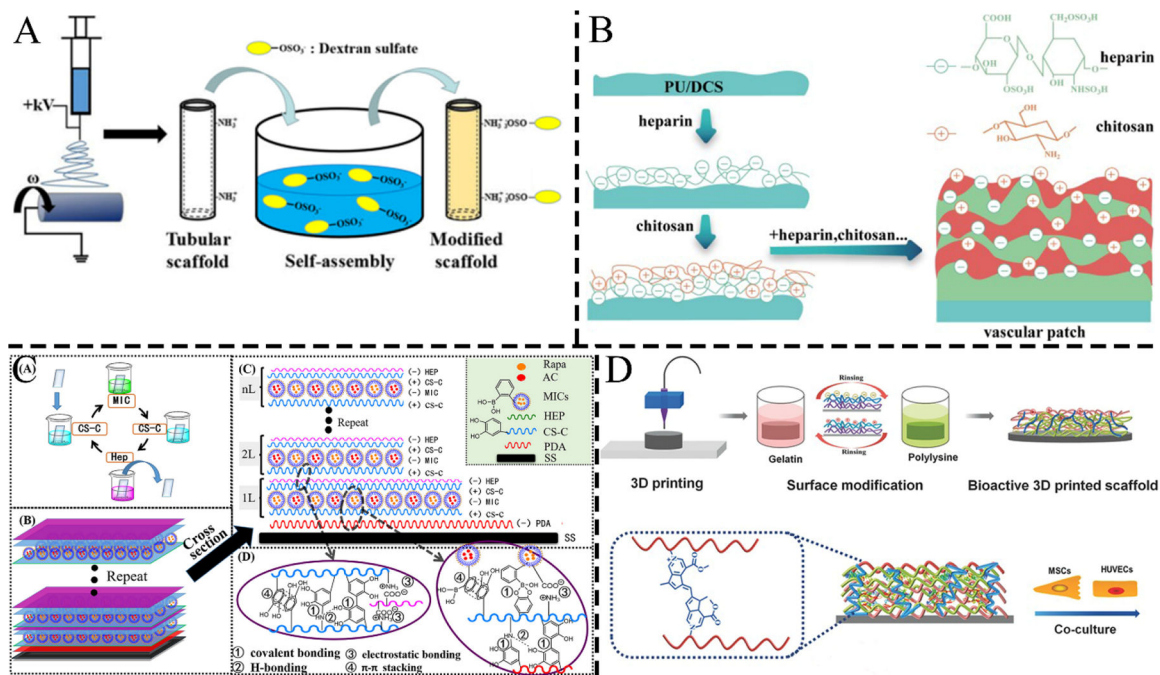


**Fig. 6.** (A) Schematic illustration of the experimental procedures for fabricating the dextran sulfate modified chitosan/poly(l-lactide-co-ε-caprolactone) (PLCL) tubular scaffold. (B) Schematic of the preparation of a multi-structured vascular patch via the LbL self-assembly of heparin and chitosan. (C) Schematic of a sandwiched LbL coating with catechol and phenylboronic acid for tunable drug loading, sustained release, and selective cell fate for re-endothelialization. (D) Schematic illustration of the fabrication process of nanocoating-modified 3D bioprinted scaffolds. (A–D) were reprinted with permission from Ref. 152: Copyright (2019) Elsevier, Ref. 37: Copyright (2019) Elsevier, Ref. 36: Copyright (2019) ACS Publications, and Ref. 16: Copyright (2016) Wiley Online Library, respectively.



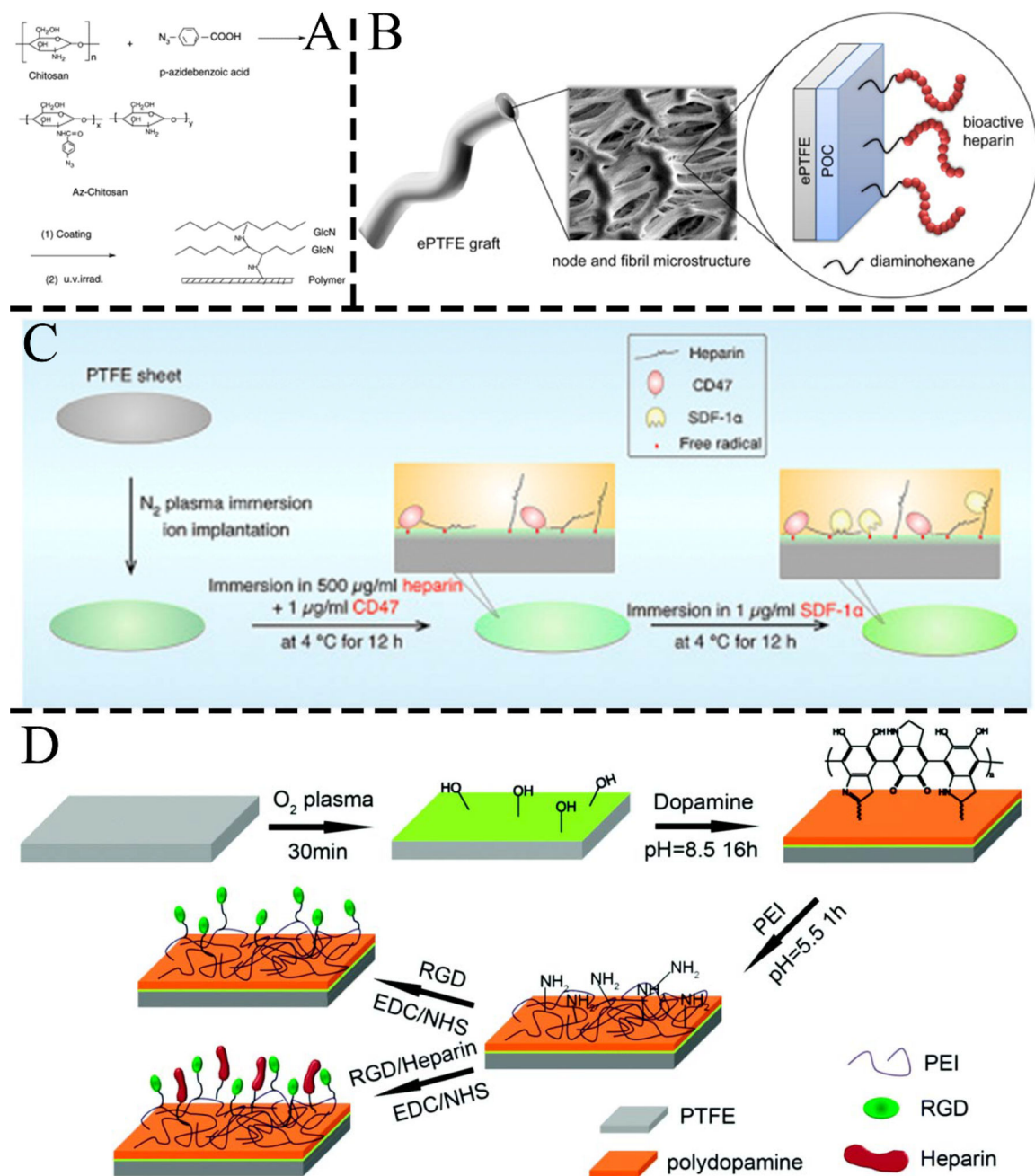


**Fig. 7.**

(A) Reaction scheme of the immobilization of chitosan on an ePTFE surface. (B) Schematic of the bioactive poly(1,8-octanediol-co-citrate)-heparin ePTFE vascular graft. (C) Schematic illustration of the covalently immobilized heparin, CD47, and SDF-1 $\alpha$  by interacting with free radicals, and SDF-1 $\alpha$  conjugated to heparin by affinity binding. (D) Stepwise surface modification procedure of PTFE, including  $O_2$  plasma treatment, dopamine coating, polyethylenimine (PEI) immobilization, and grafting of RGD or RGD/heparin. (A–D) were reprinted with permission from Ref. 136: Copyright (2005) Elsevier, Ref. 92:

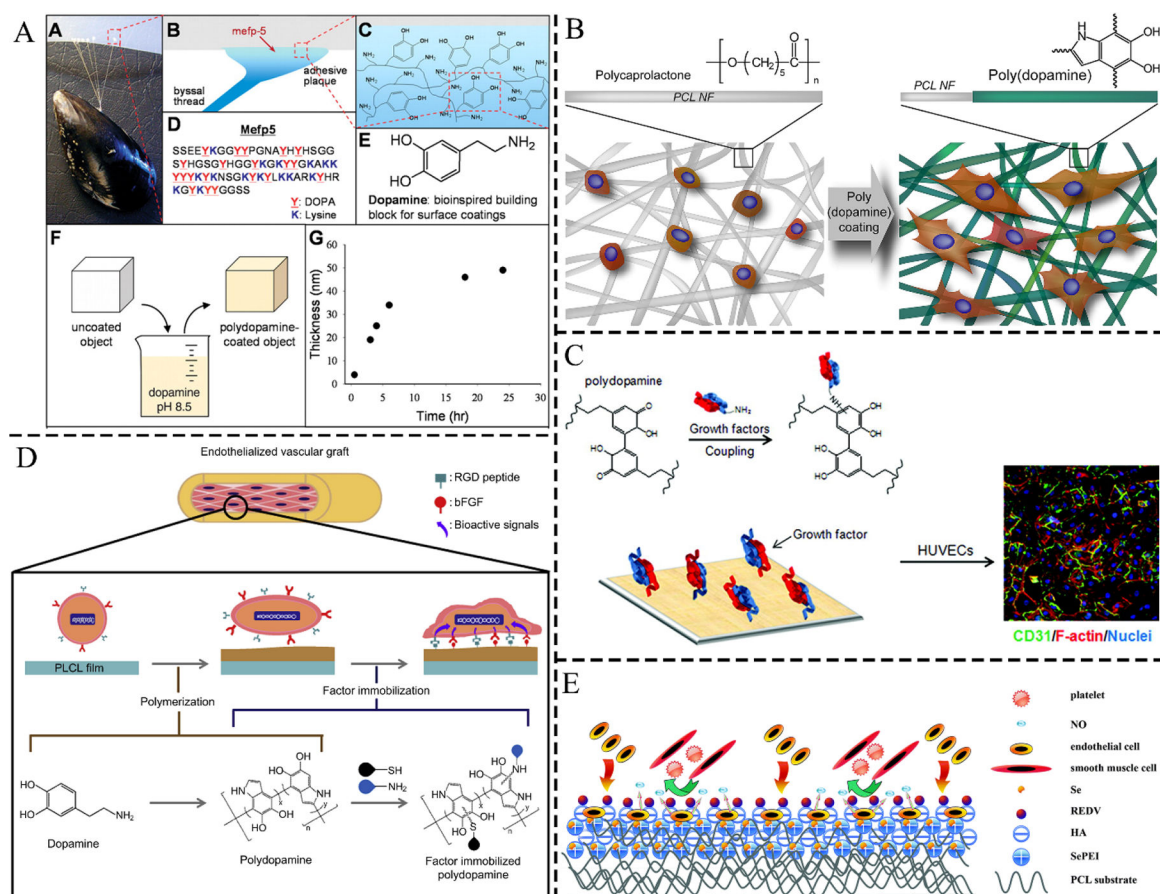
Copyright (2013) Elsevier, Ref. 5: Copyright (2017) Elsevier, and Ref. 135: Copyright (2018) Royal Society of Chemistry, respectively.

Author Manuscript

Author Manuscript

Author Manuscript

Author Manuscript

**Fig. 8.**

(A) Mussel-inspired surface chemistry for dopamine coatings. (B) Schematic illustration of cell adhesion on PDA-coated PCL nanofibers. (C) Schematic diagram of polydopamine-mediated immobilization of bioactive molecules onto PLCL films that can be utilized as a functionalized vascular graft material. (D) Schematic diagram of a surface modification using the polydopamine coating method. (E) Construction of a vascular graft loaded with SePEI and REDV for catalytic NO generation and rapid endothelialization. (A–E) were reprinted with permission from Ref. 138: Copyright (2007) Science, Ref. 48: Copyright (2010) Elsevier, Ref. 158: Copyright (2019) ACS Publications, Ref. 137: Copyright (2012) Elsevier, and Ref. 141: Copyright (2015) Royal Society of Chemistry, respectively.

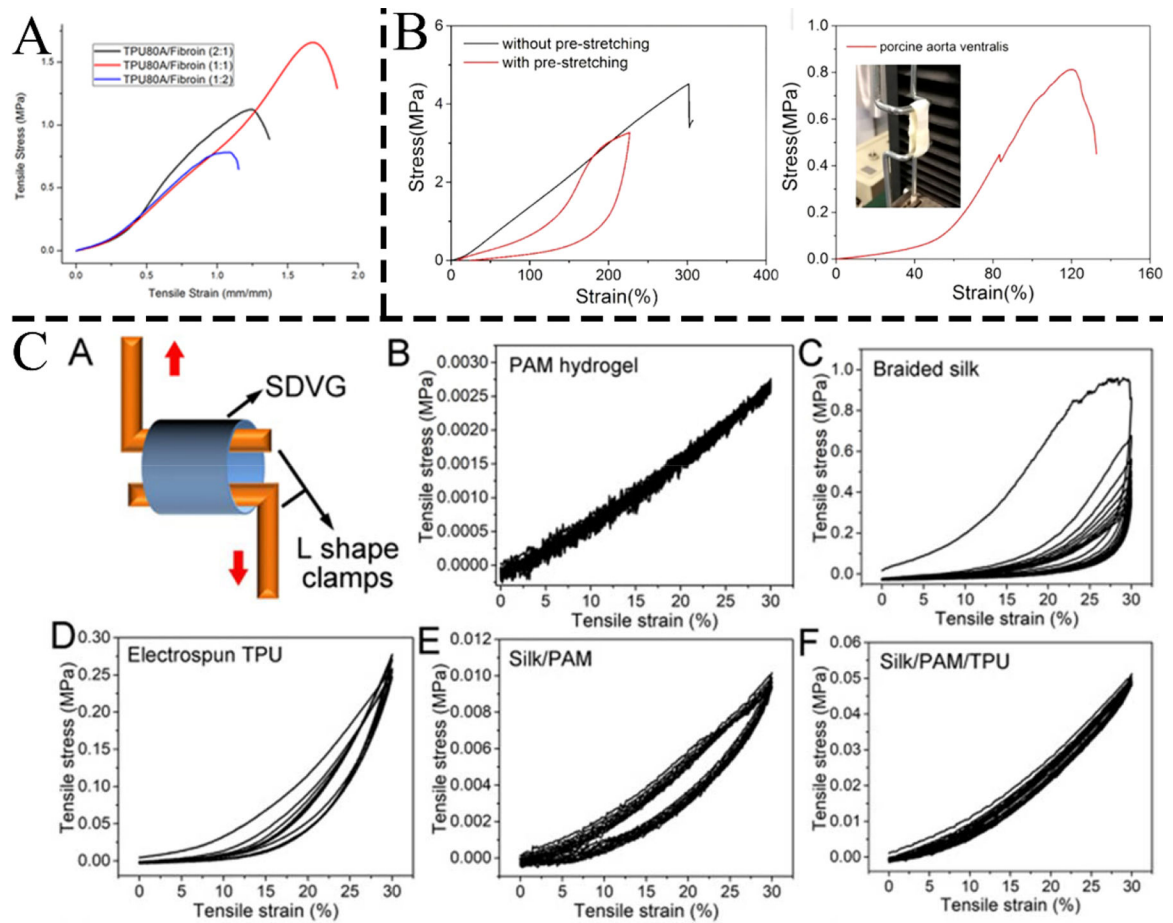


**Fig. 9.**

(A) Representative stress–strain curves of circumferential tensile tests for electrospun TPU/fibroin hybrid grafts. (B) Stress–strain curves for samples without pre-stretching (black) and loading–unloading stress–strain curves for pre-stretched samples (red), including axially aligned orientation and the stress–strain curves of porcine aorta ventralis. (C) Mechanical properties of triple-layered vascular grafts, including an illustration of the measurement method for tensile properties in the circumferential direction, and cyclic tensile properties of PAM hydrogel, braided silk, electrospun TPU, silk/PAM, and silk/PAM/TPU vascular grafts. (A–C) were reprinted with permission from Ref. 109: Copyright (2018) Wiley Online Library, Ref. 165: Copyright (2019) IOPSCIENCE, and Ref. 43: Copyright (2019) Elsevier, respectively.

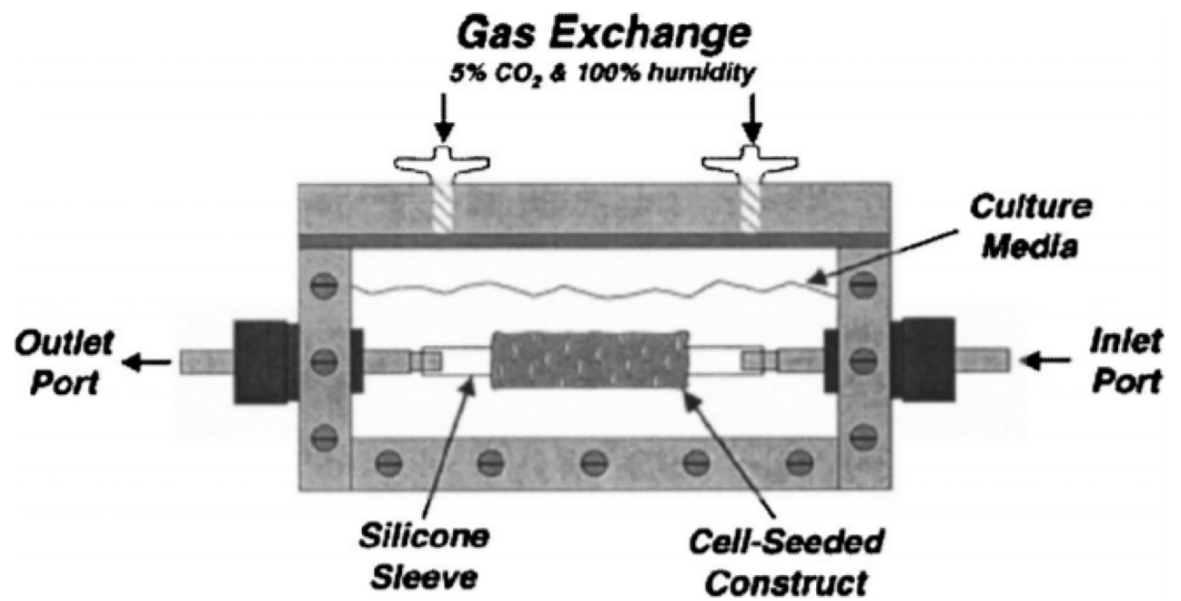


**Fig. 10.** Biomimetic bioreactor for blood vessel tissue engineering. Fig. 10 was reprinted with permission from Ref. 187: Copyright (2000) Springer.

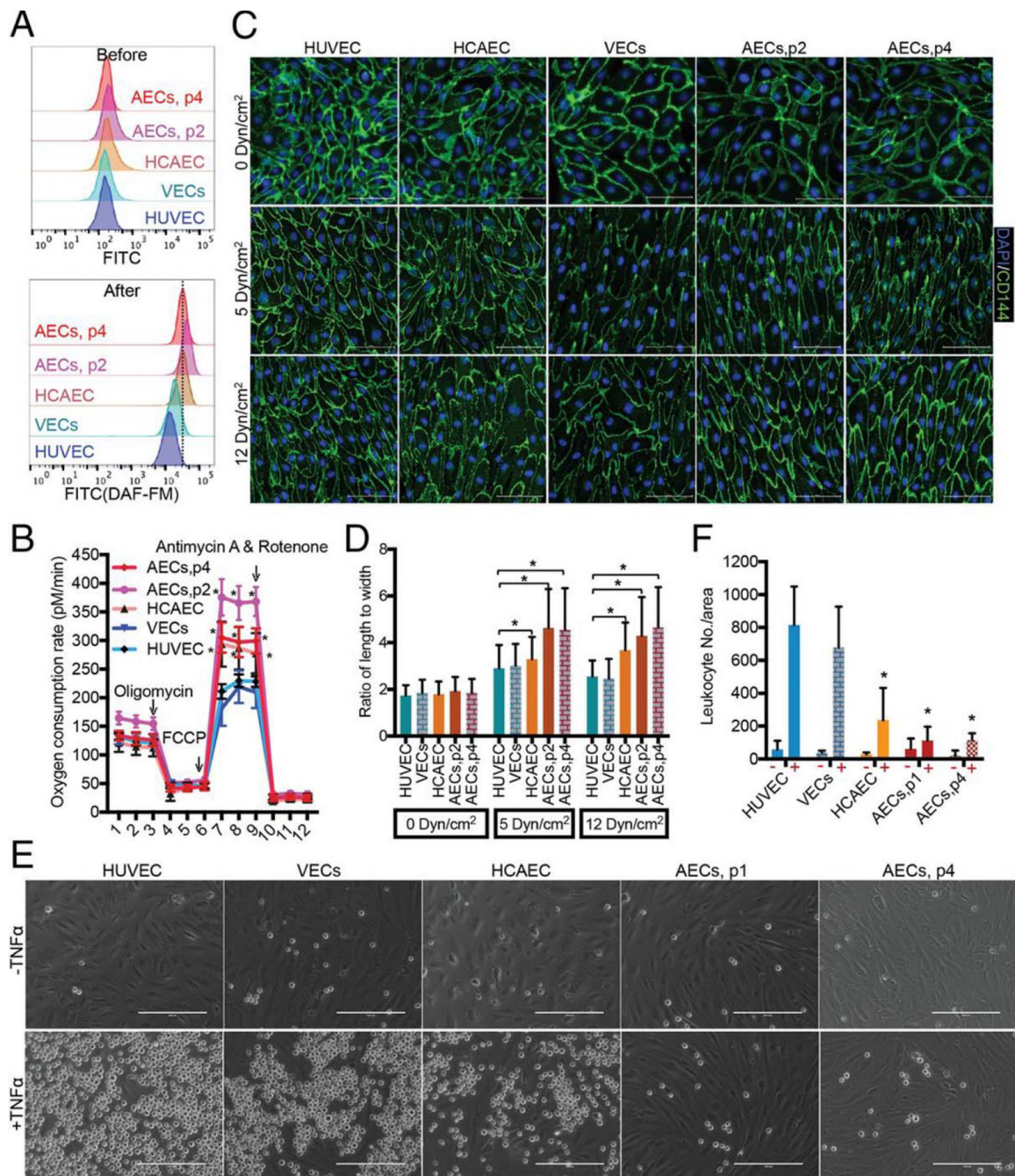


**Fig. 11.** Arterial-specific functional characterization of endothelial cells. (A) NO production test. (B) Oxygen consumption rate. (C) Shear stress response. (D) Ratio of cell length to width. (E) Leukocyte (round cells) adhesion assay. (F) Leukocyte number per unit area. Fig. 11 was reprinted with permission from Ref. 189: Copyright (2018) PNAS.

Table 1.

Several kinds of natural and synthetic polymers used for small-diameter artificial blood vessels engineered *in vitro*.

Natural Polymers	Chemical Structures	Main Advantages & Applications
Cellulose		Mechanical properties, <sup>34</sup> shape-memory, self-rolling <sup>26</sup>
Collagen		Cell adhesion, <sup>35</sup> elastic modulus, <sup>31</sup> hydrogel <sup>7</sup>
Chitosan		Cell encapsulating <sup>6</sup> surface modification <sup>37</sup>
Gelatin		Cell growth, <sup>38</sup> cell proliferation, <sup>30</sup> hydrogel, <sup>39</sup> ECM <sup>40</sup>
Silk		Biocompatibility, <sup>41</sup> compliance, <sup>42</sup> hydrogel <sup>43</sup>
Synthetic Polymers	Structural Units	Main Advantages & Applications
Gelatin methacrylate (GelMA)		Hydrogel, <sup>44</sup> cell encapsulation <sup>45</sup>
Polyacrylamide (PAM)		Hydrogel <sup>43</sup>
Poly (D,L-lactic acid-co-glycolic acid) (PLGA)		Tissue engineering and biocompatibility, <sup>46</sup> cell affinity <sup>47</sup>
Poly (ε-caprolactone) (PCL)		Tissue engineering <sup>13,48,49</sup>
Poly (ethylene glycol) (PEG)		Surface modification, <sup>50</sup> biocompatibility <sup>51</sup>
Poly (glycerol sebacate) (PGS)		Elastomer <sup>52,53</sup>

Natural Polymers	Chemical Structures	Main Advantages & Applications
Polyglycolic acid (PGA)		Thermoplastic polymer <sup>54</sup>
Poly(lactic acid) (PLA)		Mechanical properties, <sup>55</sup> tissue engineering <sup>56</sup>
Poly (L-lactic acid) (PLLA)		Mechanical properties, <sup>55</sup> tissue engineering <sup>56</sup>
Polyethylene terephthalate (PET)		Biofabrication <sup>8</sup>
Polyorthoester (POE)		Mechanical properties <sup>57</sup>
Polytetrafluoroethylene (PTFE)		Clinical reference, <sup>58</sup> surface modification <sup>5,59,60</sup>
Polyurethane (PU)		Elastomer, elastic modulus <sup>38,43</sup>
Polyvinyl alcohol (PVA)		Hydrogel <sup>61</sup>
Thermoplastic polyurethane (TPU)		Tissue engineering <sup>33</sup>



**Table 2.**

Degradation period of commonly used biodegradable polymers for SDBV fabrication.

<b>Material</b>	<b>Degradation period</b>	<b>References</b>
PGA	1 – 2 months	73,76
PCL	2 – 18 months	71,72
PLA	6 – 8 months	77,79
TPU	6 – 24 months	80
PGS	1 – 2 months	69,74
PLGA	2 – 6 months	70,78
Collagen	5 hours	75

Author Manuscript

Author Manuscript

Author Manuscript

Author Manuscript

**Table 3.**

Surface modification techniques of natural and synthetic polymers for biomedical applications.

Surface Modification Method	Surface Immobilized Agent	Biological Functions
Physical immobilization	Gelatin	Cell adhesion, <sup>48</sup> cell growth and differentiation <sup>30</sup>
	Heparin	Anticoagulation, <sup>135</sup> blood compatibility <sup>136</sup>
	RGD	Cell adhesion, <sup>135</sup> re-endothelialization <sup>137</sup>
	mPEG	Polycation, <sup>7</sup> re-endothelialization <sup>50</sup>
	Chitosan	Biocompatibility <sup>51</sup>
Surface adsorption	Dopamine	Nanocoating, <sup>56,138</sup> adhesion <sup>48,135</sup>
	Heparin	Polyanion, <sup>37</sup> antithrombogenicity <sup>139</sup>
	VEGF	EC angiogenesis <sup>30</sup>
	Collagen	Cell adhesion, <sup>28,47</sup> cell encapsulation <sup>9</sup>
Plasma treatment	Heparin	Anticoagulation, <sup>18,140</sup> endothelialization <sup>36</sup>
	REDV	Re-endothelialization, <sup>141</sup> inhibit HSMCs adhesion <sup>22</sup>
	RGD	Cell adhesion, <sup>60</sup> re-endothelialization <sup>135</sup>
	SDF-1 $\alpha$	Cell proliferation <sup>5</sup>
	VEGF	Re-endothelialization, <sup>23</sup> cell proliferation <sup>142</sup>
	YIGSR	HUVECs adhesion <sup>50</sup>
Chemical immobilization	Selenocystamine	Nitric oxide (NO) release <sup>143-145</sup>
	Cu <sup>2+</sup>	NO release and re-endothelialization <sup>146</sup>
	CD47	Cell migration <sup>5</sup>
	SDF-1 $\alpha$	Hemocompatibility and endothelialization, <sup>5</sup> cell recruitment <sup>52</sup>
	Heparin	Inhibit platelet adhesion, <sup>135</sup> anticoagulation <sup>5,31,147</sup>
	VEGF	EC angiogenesis <sup>148</sup>
	RGD	Cell adhesion <sup>137</sup>
	YIGSR	HUVECs adhesion, and re-endothelialization <sup>50</sup>
	REDV	Cell selection, <sup>22</sup> hemocompatibility and endothelialization <sup>149</sup>